

BASIC RESEARCH PAPER

## GFRA1 promotes cisplatin-induced chemoresistance in osteosarcoma by inducing autophagy

Mihwa Kim<sup>a,b,c,†,#</sup>, Ji-Yeon Jung<sup>a,d,#</sup>, Seungho Choi<sup>a</sup>, Hyunseung Lee<sup>b,c,†</sup>, Liza D. Morales<sup>b,†</sup>, Jeong-Tae Koh<sup>d,e</sup>, Sun Hun Kim<sup>d,f</sup>, Yoo-Duk Choi<sup>g</sup>, Chan Choi<sup>g</sup>, Thomas J. Slaga<sup>c</sup>, Won Jae Kim<sup>a,d</sup>, and Dae Joon Kim<sup>b,c,†</sup>

<sup>a</sup>Department of Oral Physiology, School of Dentistry, Chonnam National University, Gwangju, Korea; <sup>b</sup>Edinburg Regional Academic Health Center, Medical Research Division, University of Texas Health Science Center at San Antonio, Edinburg, TX, USA; <sup>c</sup>Department of Pharmacology, University of Texas Health Science Center at San Antonio, San Antonio, TX, USA; <sup>d</sup>Dental Science Research Institute, Medical Research Center for Biomineralization Disorders, School of Dentistry, Chonnam National University, Gwangju, Korea; <sup>e</sup>Department of Pharmacology and Dental Therapeutics, School of Dentistry, Chonnam National University, Gwangju, Korea; <sup>f</sup>Department of Oral Anatomy, School of Dentistry, Chonnam National University, Gwangju, Korea; <sup>g</sup>Department of Pathology, Chonnam National University Medical School, Gwangju, Korea

### ABSTRACT

Recent progress in chemotherapy has significantly increased its efficacy, yet the development of chemoresistance remains a major drawback. In this study, we show that GFRA1/GFR $\alpha$ 1 (GDNF family receptor  $\alpha$  1), contributes to cisplatin-induced chemoresistance by regulating autophagy in osteosarcoma. We demonstrate that cisplatin treatment induced GFRA1 expression in human osteosarcoma cells. Induction of GFRA1 expression reduced cisplatin-induced apoptotic cell death and it significantly increased osteosarcoma cell survival via autophagy. GFRA1 regulates AMPK-dependent autophagy by promoting SRC phosphorylation independent of proto-oncogene *RET* kinase. Cisplatin-resistant osteosarcoma cells showed NFKB1/NF $\kappa$ B-mediated GFRA1 expression. GFRA1 expression promoted tumor formation and growth in mouse xenograft models and inhibition of autophagy in a GFRA1-expressing xenograft mouse model during cisplatin treatment effectively reduced tumor growth and increased survival. In cisplatin-treated patients, treatment period and metastatic status were associated with GFRA1-mediated autophagy. These findings suggest that GFRA1-mediated autophagy is a promising novel target for overcoming cisplatin resistance in osteosarcoma.

### ARTICLE HISTORY

Received 14 October 2015  
Revised 13 September 2016  
Accepted 19 September 2016

### KEYWORDS

AMPK; autophagy; chemoresistance; GFRA1; osteosarcoma; SRC

### Introduction

Osteosarcoma is the predominant form of primary bone cancer. It is a highly malignant tumor that mostly arises in childhood and adolescence.<sup>1</sup> Use of chemotherapy along with surgery has raised the long-term survival rate of osteosarcoma patients to approximately 70%.<sup>2,3</sup> Doxorubicin, cisplatin, and methotrexate are commonly used chemotherapeutics active against osteosarcoma. In particular, cisplatin is the most widely used platinum-based anticancer drug for solid tumors including osteosarcoma.<sup>4</sup> It interacts with nucleophilic N7 sites of purine bases in DNA to induce DNA damage that leads to inhibition of tumor cell division and initiation of apoptosis, or programmed cell death.<sup>5</sup> Although this treatment strategy is highly effective, it is often limited by acquired or intrinsic resistance of cancer cells to the drug.<sup>6</sup> Thus, understanding the molecular mechanisms which lead to chemoresistance is essential to developing more effective treatments against osteosarcoma.


Autophagy is a critical process by which cells self-digest and recycle inessential or ineffectual cellular components to

maintain homeostasis, especially under conditions of metabolic stress.<sup>7,8</sup> During the initial stages of autophagy, cellular proteins, organelles and cytoplasm are sequestered and engulfed by autophagosomes. The autophagosomes then fuse with lysosomes to form the autolysosomes, where the sequestered proteins and organelles are digested by lysosomal hydrolases.<sup>9,10</sup> Autophagy can play a role in cell death as an alternative cell death mechanism known as programmed cell death type II, particularly within apoptosis-deficient cells and through this mechanism it can function in tumor suppression.<sup>11–13</sup> Paradoxically, autophagy has also been established as a cell survival mechanism that is induced by environmental stresses including nutrient deficiency, chemotherapy, radiation, and hypoxia.<sup>11,12,14</sup> Induction of autophagy for cell survival can confer resistance to anticancer therapies in some cancers.<sup>15–19</sup> However, the relative contribution of autophagy to either apoptotic cell death as a tumor suppressive mechanism or cell survival mechanism remains mostly unresolved.

**CONTACT** Won Jae Kim ✉ [wjkim@jnu.ac.kr](mailto:wjkim@jnu.ac.kr) Department of Physiology, School of Dentistry, Chonnam National University, 77 Yongbong-Ro, Buk-Gu, Gwangju 61186, Korea; Dae Joon Kim ✉ [dae.kim@utrgv.edu](mailto:dae.kim@utrgv.edu) Department of Biomedical Sciences, School of Medicine, University of Texas Rio Grande Valley, 1214 W Schunior St, Edinburg, TX 78541, USA

<sup>#</sup>These authors contributed equally to this study.

<sup>†</sup>Current address: Department of Biomedical Sciences, School of Medicine, University of Texas Rio Grande Valley, Edinburg, TX, USA.

 Supplemental data for this article can be accessed on the publisher's website.

The glycosylphosphatidylinositol-linked GDNF (glial cell derived neurotrophic factor) receptor  $\alpha$ , is a coreceptor that recognizes the GDNF family of ligands, which includes GDNF, NRTN (neurturin), ARTN (armin), and PSPN (persephin).<sup>20,21</sup> Four different GFRA receptors have been identified. GFRA1/GFR $\alpha$ 1 (GDNF family receptor  $\alpha$  1) specifically recognizes GDNF and has been implicated in the regulation of neuronal cell survival and differentiation. Binding of GFRA with GDNF activates protein tyrosine kinase RET and subsequently activates SRC, a member of the SRC family of cytoplasmic tyrosine kinases.<sup>20</sup> GDNF-GFRA signaling regulates the development and maintenance of the nervous system by protecting and promoting survival of dopaminergic neurons and thereby it has potential as a therapeutic target for neurodegenerative diseases.<sup>22,23</sup> Studies also have indicated that GFRA1 has a role in the progression and metastasis of human cancers such as breast cancer and pancreatic cancer in that it promotes migration and invasion,<sup>24-27</sup> although the exact mechanism for oncogenesis remains unclear. Here, we report a novel mechanism in which GFRA1 contributes to the development of cisplatin-

induced chemoresistance in osteosarcoma by facilitating autophagy via SRC-AMP-activated protein kinase (AMPK) signaling.

## Results

### GFRA1 expression is induced by cisplatin in osteosarcoma cells

Aberrant expression of GFRA1 has been observed in malignant human cancers and it has a role in regulating tumor cell migration and invasion. To investigate whether GFRA1 has a role in chemoresistance of osteosarcoma, we first examined the effects of doxorubicin, cisplatin, and methotrexate on GFRA1 expression in 2 well-known osteosarcoma cell lines, MG-63 and U-2 OS. Cisplatin significantly increased the level of GFRA1 expression in both cell lines, whereas doxorubicin and methotrexate showed little or no effect on its expression (Fig. 1A). The effect of cisplatin on GFRA1 expression was dose and time dependent (Fig. 1B, C). Cisplatin also increased the level of *GFRA1* mRNA

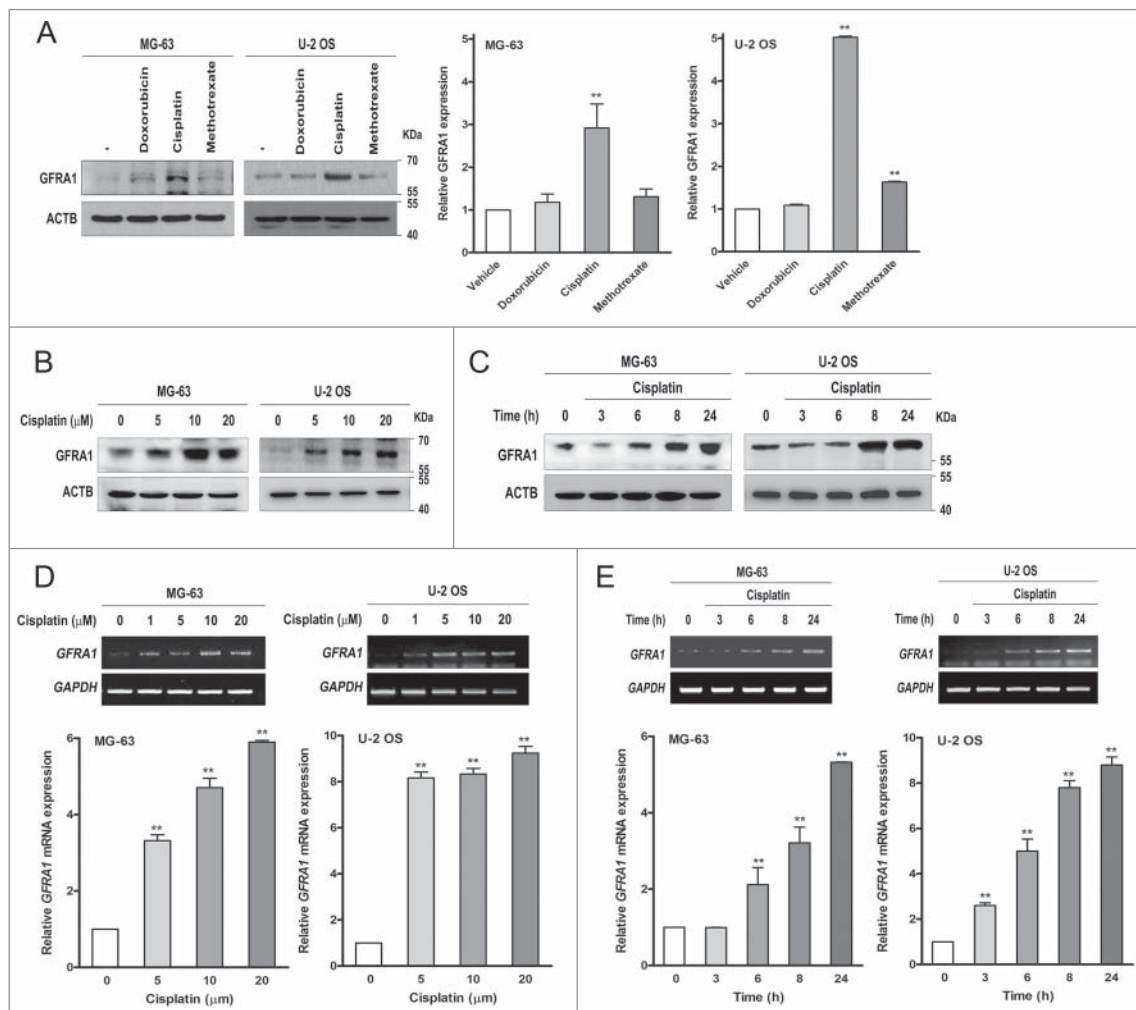


**Figure 1.** Cisplatin induces GFRA1 expression in osteosarcoma cells. (A to C) Immunoblot analysis of osteosarcoma cell lysates with antibodies specific for GFRA1 and ACTB/ $\beta$ -actin. (A) MG-63 and U-2 OS cells were treated with doxorubicin (5  $\mu$ M), cisplatin (20  $\mu$ M), or methotrexate (1 mM) for 24 h. Immunoblot analysis of GFRA1 (left) and quantification of GFRA1 expression (right) after treatment of chemotherapeutic agents. (B) MG-63 and U-2 OS cells were treated with different concentrations of cisplatin for 24 h. (C) MG-63 and U-2 OS cells were treated with cisplatin (20  $\mu$ M) and collected at the indicated time. (D and E) Quantitative real-time PCR of *GFRA1* mRNA expression after cisplatin treatment. Representative images (top) and quantitative analysis (bottom) of *GFRA1* mRNA expression. (D) MG-63 and U-2 OS cells were treated with different concentrations of cisplatin for 24 h. (E) MG-63 and U-2 OS cells were treated with cisplatin (20  $\mu$ M) and collected at the indicated time. The values are presented as a mean  $\pm$  s.d.m. (n = 3). \*\* denotes  $P < 0.05$ .

in both cell lines in a dose- and time-dependent manner (Fig. 1D, E, respectively), indicating that GFRA1 expression is induced by cisplatin at both transcriptional and translational levels. To examine the effects of GFRA1 expression on the efficacy of the chemotherapeutic agents, *GFRA1* was knocked down by *GFRA1*-specific small interfering RNA (siRNA) in both MG-63 and U-2 OS cells and then the cell lines were treated with each of the 3 agents. Cisplatin treatment significantly reduced cell proliferation in both GFRA1-deficient MG-63 and U-2 OS cells compared to control cells, whereas doxorubicin and methotrexate showed little or no effect (Fig. S1A, B). Based on these results, we utilized the optimal dose (20  $\mu$ M) and time (24 h) of cisplatin treatment for the following cell viability studies. Given that GDNF is the major ligand of GFRA1, we also examined the effect of cisplatin on GDNF expression. An increase in *GDNF* mRNA expression was detected after treatment with 10 and 20  $\mu$ M of cisplatin in osteosarcoma cells (Fig. S2A). However, GDNF had no effect on cell viability of MG-63 cells (Fig. S2B). The results imply GFRA1 inhibits cisplatin-induced apoptosis and this effect is independent of the GFRA1 ligand GDNF.

### **GFRA1 expression reduces efficacy of cisplatin in osteosarcoma cells**

To further investigate the role of GFRA1 in cisplatin-induced apoptosis, we generated stable GFRA1-deficient MG-63 and U-2 OS cell lines using *GFRA1*-specific small hairpin RNA (shRNA). Knockdown of *GFRA1* expression led to a decrease of GFRA1 protein levels in both osteosarcoma cell lines compared to control cells after cisplatin treatment (Fig. 2A). Like siRNA-mediated knockdown of *GFRA1*, stable knockdown of *GFRA1* significantly reduced cell proliferation of cisplatin-treated osteosarcoma cells in a dose-dependent manner compared to control cells (Fig. 2B). Furthermore, knockdown of *GFRA1* significantly increased cisplatin-induced apoptosis which corresponded with a significant reduction in cell viability (Fig. 2C and Fig. S3A, S4A). Western blot analysis with the apoptotic markers PARP1 (poly[ADP-ribose] polymerase) and CASP3/caspase-3 confirmed this result as evidenced by a significant increase in both cleaved PARP and cleaved CASP3 expression levels in both GFRA1-deficient MG-63 and U-2 OS cells after cisplatin treatment (Fig. 2D). Consistently, CASP3 activity significantly increased in both GFRA1-deficient cells, and it increased even more dramatically upon treatment with cisplatin in both GFRA1-deficient cells compared to cisplatin-treated control cells (Fig. 2E). Addition of the pancaspase inhibitor Z-VAD-FMK reversed this effect (Fig. 2E), indicating loss of GFRA1 stimulates apoptosis, particularly in the presence of cisplatin. Additionally, we generated stable MG-63 and U-2 OS cell lines that overexpress human GFRA1 by transfection with a human *GFRA1* expression vector (Fig. 2F). Overexpression of GFRA1 did not lead to an increase in cell proliferation of either cisplatin-treated osteosarcoma cell line in dose response experiments (Fig. 2G). However, further analysis using FACS showed that overexpression of GFRA1 significantly reduced cisplatin-induced apoptosis which corresponded with an increase in cell viability in both cell lines (Fig. 2H and Fig. S3B, S4B). Addition of GDNF had no

significant effect on cell viability in control or GFRA1-overexpressing cells in the presence or absence of cisplatin (Fig. S2C, D). Together, these results demonstrate that GFRA1 reduces the susceptibility of osteosarcoma cells to cisplatin-induced apoptosis.

### **GFRA1 triggers autophagy in osteosarcoma cells in response to cisplatin**

Autophagy is a mechanism that can promote resistance to apoptosis and potentially chemotherapy, which works by triggering cell death. Therefore, we assessed what role autophagy might play in cisplatin-induced apoptosis of osteosarcoma cells in relation to GFRA1 expression. We first investigated whether GFRA1 deficiency regulates MAP1LC3/LC3 (microtubule-associated protein 1 light chain 3) puncta formation, which is widely used as a marker for autophagy.<sup>28</sup> We examined the effect of the dose and time of cisplatin treatment on autophagy and found the ratio of LC3-II to LC3-I was increased in a dose- and time-dependent manner (data not shown). Based on these results, we utilized the optimal dose (20  $\mu$ M) and time (24 h) of cisplatin treatment for studying autophagy. Fluorescent imaging analysis of LC3 puncta formation using an *mRFP-GFP-LC3* reporter showed that cisplatin treatment significantly increased LC3 puncta formation in MG-63 cells transfected with control shRNA, while there was no change in puncta formation in GFRA1-deficient cells (Fig. 3A). Cisplatin treatment increased both mRFP- and GFP-positive yellow puncta (autophagosomes) and mRFP-positive red puncta (autolysosomes) formation in control cells, though the number of mRFP- and GFP-positive yellow puncta was greater than the number of mRFP-positive red puncta (Fig. 3A). Acridine orange staining of GFRA1-deficient MG-63 cells or GFRA1-deficient U-2 OS cells showed that knockdown of *GFRA1* did not increase the accumulation of acidic vesicular organelle (AVO)-positive cells following cisplatin treatment, while control cells showed a significant increase in AVO-positive cells with cisplatin (Fig. 3B and Fig. S5A, respectively). Moreover, ultrastructural analysis by transmission electron microscopy (TEM) revealed that the number of autophagic vacuoles per cell was markedly increased in control cells following cisplatin treatment, whereas GFRA1 deficiency had no effect on autophagic vacuole formation (Fig. 3C). Addition of 3-methyladenine (3-MA), an inhibitor of early-phase autophagy, blocked cisplatin-induced puncta formation in MG-63 cells (Fig. 4A). To further confirm cisplatin-induced autophagy, we generated a stable BECN1/Beclin 1-deficient MG-63 cell line using *BECN1*-specific shRNA. Knockdown of *BECN1* expression led to a decrease of BECN1 protein levels in MG-63 cells (Fig. 4B). Similar to 3-MA treatment, stable knockdown of *BECN1* significantly reduced puncta formation after cisplatin treatment compared to cisplatin treated control cells (Fig. 4C). The data suggests that cisplatin induces autophagy in osteosarcoma and GFRA1 is required for this autophagic response.

To further investigate the involvement of GFRA1 in cisplatin-induced autophagy, we examined the conversion of LC3-I to LC3-II which occurs during autophagosome formation.<sup>9,11,12,29</sup> Western blot analysis showed an increase in the

level of LC3-II protein production in GFRA1-overexpressing MG-63 cells in comparison to control (Fig. 4D). Addition of 3-MA reduced the level of LC3-II production, whereas bafilomycin A1 (Baf), an inhibitor of late-phase autophagy, increased LC3-II production levels (Fig. 4D). Consistent with these results, LC3 puncta formation following cisplatin treatment was increased in both GFRA1-overexpressing MG-63 and U-2

OS cells compared to control cells (Fig. 4E and Fig. S2E). Whereas the number of mRFP- and GFP-positive yellow puncta was greater than the number of mRFP-positive red puncta in cisplatin-treated control cells, the number of mRFP-positive red puncta was much greater than the number of mRFP- and GFP-positive yellow puncta in GFRA1-overexpressing cells (Fig. 4E and Fig. S2E), suggesting that GFRA1

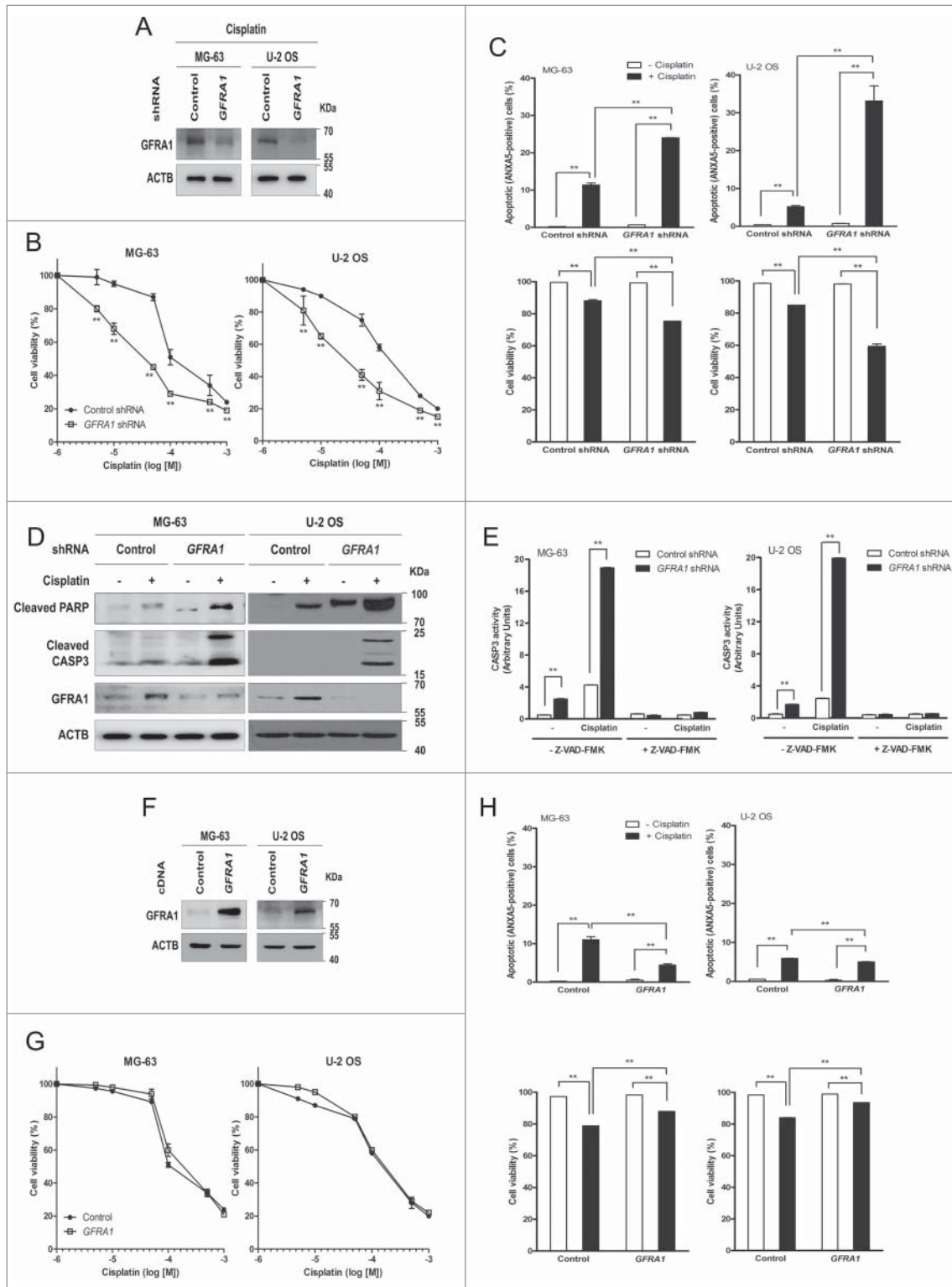


Figure 2. (For figure legend, see page 153.)

increases autophagic flux. It is important to note that basal LC3 puncta formation without cisplatin treatment was also higher in GFRA1-overexpressing cells compared to control cells (Fig. 4E and Fig. S2E). Treatment with 3-MA blocked puncta formation in both control and GFRA1-overexpressing cells (Fig. 4F and Fig. S2E). LC3 puncta formation was also significantly reduced in BECN1-deficient, GFRA1-overexpressing MG-63 cells compared to GFRA1-overexpressing cells (Fig. 4G). Addition of GDNF had no significant effect in either control or GFRA1-overexpressing cells (Fig. S2E, S2F). Consistently, GFRA1 overexpression in osteosarcoma cells increased AVO-positive cells compared to control cells with or without cisplatin treatment (Fig. 5A and Fig. S5B). The number of autophagic vacuoles per cell also was significantly increased in GFRA1-overexpressing cells compared to control cells with or without cisplatin treatment (Fig. 5B).

Previous work showed that APEX1/APE1 (apurinic/apyrimidinic endodeoxyribonuclease 1) can increase GDNF responsiveness by upregulating GFRA1 expression in pancreatic cancer cells<sup>27</sup> so we examined whether APEX1 is involved in GFRA1-mediated autophagy in osteosarcoma cells. Western blot analysis showed that APEX1 expression levels were not affected by cisplatin treatment (Fig. S6A). Moreover, knockdown of *APEX1* in MG-63 cells did not reduce the level of LC3-II production and AVO-positive cells compared to control cells after cisplatin treatment (Fig. S6B, S6C). We also examined whether RET, the downstream kinase activated by of the GDNF-GFRA1 complex, is involved in GFRA1-mediated autophagy. Western blot analysis showed that RET expression was not detected in osteosarcoma cells (Fig. S6A). The results indicate that APEX1 and RET are not involved in GFRA1-mediated autophagy.

Cell proliferation in GFRA1-overexpressing cells was significantly higher in the presence or absence of cisplatin compared to control cells which correlates with the increase of autophagy observed in GFRA1-overexpressing cells and this effect was blocked by addition of 3-MA but not by Baf and chloroquine (CQ) (Fig. 5C). The increase in cell proliferation observed in GFRA1-overexpressing cells was also blocked by silencing the autophagy proteins BECN1 or HMGB1 with siRNA (Fig. 5D), supporting that induction of GFRA1-mediated autophagy by cisplatin contributes to increased cell proliferation.

To demonstrate GFRA1-mediated autophagy promotes cell viability and thereby chemoresistance, control cell lines, GFRA1-deficient, stable cell lines or GFRA1-overexpressing, stable cell lines were cultured in the presence of cisplatin and

the resultant colonies were counted. All 4 cell lines overexpressing GFRA1 developed a significant number of colonies after 7 d of incubation and showed high plating efficiency, whereas none of the control cell lines nor the GFRA1-deficient cell lines developed colonies (Fig. 6A). Treatment of GFRA1-overexpressing MG-63 clone #4, which appeared to be highly resistant to cisplatin, with 3-MA, Baf, or CQ revealed that inhibition of autophagy effectively reduced the number of colonies and viability formation mediated by GFRA1 (Fig. 6B). The data suggests GFRA1 triggers autophagy to promote cisplatin resistance.

### GFRA1 transcriptional regulator NFKB1 is upregulated in cisplatin-resistant osteosarcoma cells

We also generated 3 cisplatin-resistant MG-63 clones by treating MG-63 cells with cisplatin for 10 d. Consistently, all 3 cisplatin-resistant cell lines developed much higher numbers of colonies compared to control MG-63 cells (Fig. 7A, B). Furthermore, the level of *GFRA1* mRNA expression was significantly increased in these cell lines compared to control (Fig. 7C).

The transcription factor NFKB1/NFκB is able to bind the GFRA1 gene promoter and subsequently upregulate *GFRA1* mRNA expression.<sup>27</sup> Consistent with this data, the level of *NFKB1* mRNA expression was also significantly increased in the cisplatin-resistant cell lines compared to control cells (Fig. 7D). Knockdown of *NFKB1* with siRNA reduced the level of *GFRA1* mRNA expression in MG-63 cells (Fig. 7E, F), implying cisplatin may activate NFKB1 in order to stimulate expression of GFRA1 for the activation of autophagy and cell survival. Consistent with these results, the expression levels of GFRA1, NFKB1, and phosphorylated NFKB1 were increased in cisplatin-treated MG-63 cells compared to untreated controls (Fig. 7G). Similarly, their expression levels were higher in cisplatin-resistant cell lines compared to control MG-63 cells after cisplatin treatment (Fig. 7H). Knockdown of *NFKB1* with siRNA reduced the level of GFRA1 expression in cisplatin-resistant cell clone #2 (MG-63-CIS<sup>R</sup>-2) (Fig. 7I).

### GFRA1 regulates autophagy through SRC-AMPK signaling

SRC is activated by GFRA1-RET signaling.<sup>20</sup> SRC also is activated by GFRA1 in RET-deficient cells, indicating GFRA1 can activate SRC signaling in a RET-independent manner.<sup>20,30</sup> In addition to its oncogenic functions in a variety of cancers, SRC can function in autophagy.<sup>31,32</sup> For example, AMPK activation

**Figure 2.** (see previous page) GFRA1 suppresses the chemosensitivity of osteosarcoma cells induced by cisplatin. (A) Generation of GFRA1-deficient osteosarcoma cell lines with *GFRA1* shRNA. Both MG-63 and U-2 OS cells were transfected with control or *GFRA1* shRNA and treated with cisplatin (20 μM) for 24 h. Immunoblot analysis of control and GFRA1-deficient stable osteosarcoma cell lysates with antibodies specific for GFRA1 and ACTB. (B) Cell viability of GFRA1-deficient osteosarcoma cells after cisplatin treatment. Control or GFRA1-deficient cells were cultured and treated with different concentrations of cisplatin for 24 h. Cell viability was measured using the WST-1 assay. (C) Apoptotic response of GFRA1-deficient osteosarcoma cells after cisplatin treatment. Control and GFRA1-deficient cells were cultured and treated with cisplatin (20 μM) for 24 h. Apoptotic cells by ANXA5 and FITC staining (top) and viable cells by PI staining (bottom) were analyzed through flow cytometry. (D) Immunoblot analysis of control and GFRA1-deficient osteosarcoma cell lysates with antibodies specific for apoptotic proteins, cleaved PARP and cleaved CASP3. Control and GFRA1-deficient osteosarcoma cells were treated with cisplatin (20 μM) for 24 h and cells were collected. (E) Relative CASP3 activity in control and GFRA1-deficient osteosarcoma cells after cisplatin treatment. Control and GFRA1-deficient osteosarcoma cells were treated with cisplatin (20 μM) for 24 h in the presence or absence of Z-VAD-FMK (50 μM). (F) Generation of GFRA1-overexpressing osteosarcoma cell lines with *GFRA1* expression vector. Both MG-63 and U-2 OS cells were transfected with control or human *GFRA1* expression vector. Immunoblot analysis of control and GFRA1-overexpressing stable osteosarcoma cell lysates with antibodies specific for GFRA1 and ACTB. (G) Cell viability of GFRA1-overexpressing osteosarcoma cells after cisplatin treatment. Control and GFRA1-overexpressing cells were cultured and treated with different concentrations of cisplatin for 24 h. Cell viability was measured using the WST-1 assay. (H) Apoptotic response of GFRA1-overexpressing osteosarcoma cells after cisplatin treatment. Control and GFRA1-overexpressing cells were cultured and treated with cisplatin (20 μM) for 24 h. Apoptotic cells by ANXA5 and FITC staining (top) and viable cells by PtdIns staining (bottom) were analyzed through flow cytometry. The values are presented as a mean ± s.d.m. (n = 3). \*\* denotes  $P < 0.05$ .

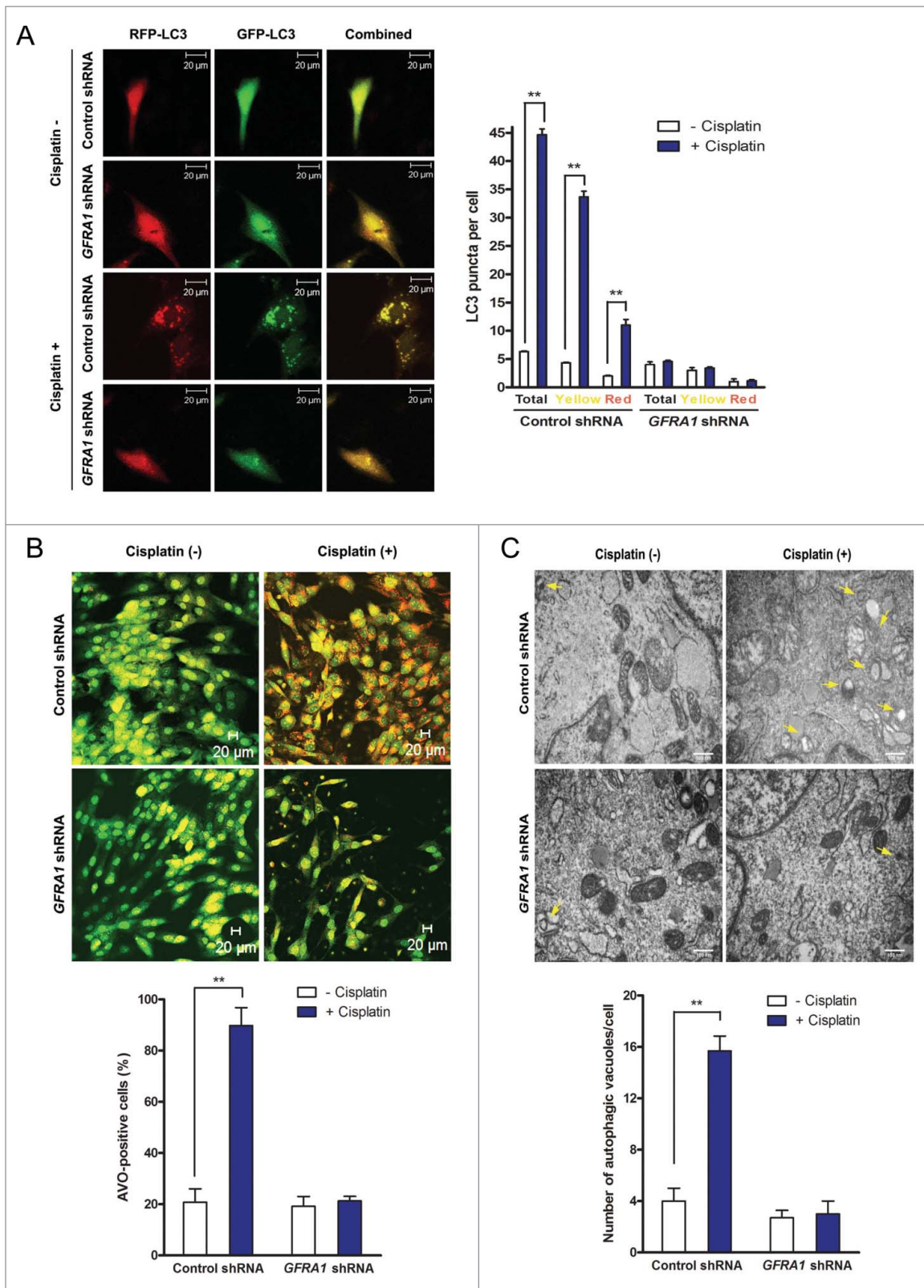


**Figure 3.** GFRA1 deficiency reduces autophagy in osteosarcoma cells induced by cisplatin. (A) Control and GFRA1-deficient MG-63 cells were transiently transfected with an mRFP-GFP tandem fluorescent-tagged LC3 (*mRFP-GFP-LC3*) vector and then treated with cisplatin ( $20 \mu\text{M}$ ) for 24 h. Left, representative images of mRFP-LC3 and GFP-LC3 puncta. Scale bar:  $20 \mu\text{m}$ . Right, quantitative analysis of the number of yellow puncta and the number of mRFP-LC3 puncta in the combined images. (B) Control and GFRA1-deficient MG-63 cells were treated with cisplatin ( $20 \mu\text{M}$ ) for 24 h and then stained with acridine orange. Top, representative images of cells stained with acridine orange. Scale bar:  $20 \mu\text{m}$ . Bottom, quantitative analysis of the number of AVOs. (C) Control and GFRA1-deficient MG-63 cells were treated with cisplatin ( $20 \mu\text{M}$ ) for 24 h and then analyzed by TEM. Top, representative images of autophagic vacuoles (yellow arrows) detected after cisplatin treatment in control MG-63 cells. Scale bar:  $100 \text{ nm}$ . Bottom, quantitative analysis of the number of autophagic vacuoles.

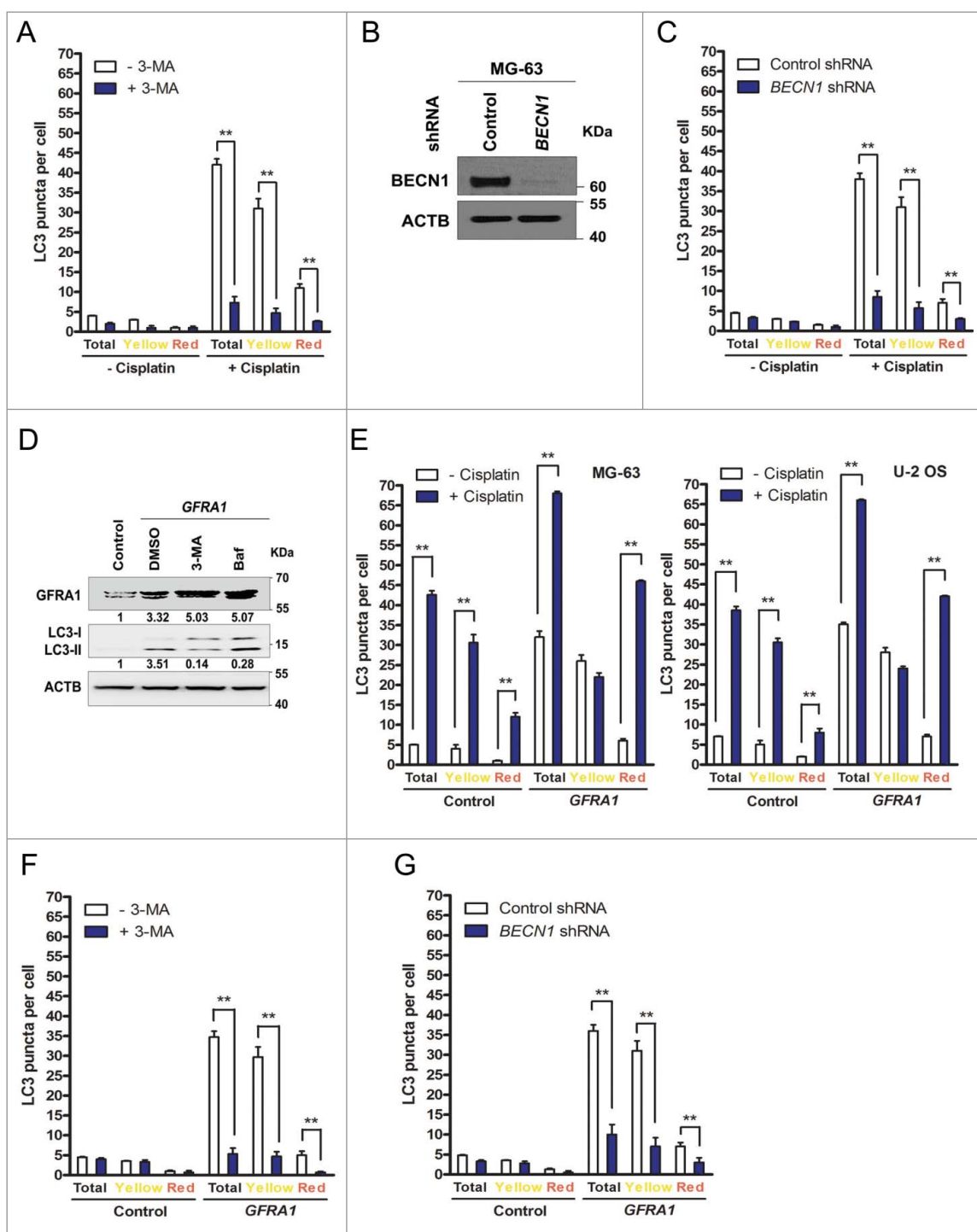


**Figure 4.** Inhibition of autophagy reduces puncta formation in osteosarcoma cells induced by cisplatin. (A) MG-63 cells were pretreated with 3-MA (10 mM) for 2 h before *mRFP-GFP-LC3* transfection and were then treated with cisplatin (20  $\mu$ M) for 24 h. (B) Generation of BECN1-deficient osteosarcoma cell line with *BECN1* shRNA. MG-63 cells were transfected with control or *BECN1* shRNA. Immunoblot analysis of control and BECN1-deficient stable osteosarcoma cell lysates with antibodies specific for BECN1 and ACTB. (C) Control and BECN1-deficient MG-63 cells were transiently transfected with an mRFP-GFP tandem fluorescent-tagged LC3 (*mRFP-GFP-LC3*) vector and then treated with cisplatin (20  $\mu$ M) for 24 h. (D) Immunoblot analysis of control and GFRA1-overexpressing osteosarcoma cell lysates with antibodies specific for GFRA1, LC3 and ACTB. GFRA1-overexpressing MG-63 cells were treated with DMSO, 3-MA (10 mM) or Baf (100 nM). The numbers below the lanes indicate densitometric quantification of GFRA1 and LC3-II to LC3-I ratios relative to the ACTB control. (E) Quantitative analysis of the number of yellow puncta and the number of mRFP-LC3 puncta in control and GFRA1-overexpressing MG-63 cells. Control and GFRA1-overexpressing MG-63 cells were transiently transfected with an mRFP-GFP tandem fluorescent-tagged LC3 (*mRFP-GFP-LC3*) and then treated with cisplatin (20  $\mu$ M) for 24 h. (F) Control and GFRA1-overexpressing MG-63 cells were pretreated with 3-MA (10 mM) for 2 h before *mRFP-GFP-LC3* transfection and were then incubated for 24 h. (G) Control, GFRA1-overexpressing, and BECN1-deficient/GFRA1-overexpressing MG-63 cells were transiently transfected with an RFP-GFP tandem fluorescent-tagged LC3 (*mRFP-GFP-LC3*) and then treated with cisplatin (20  $\mu$ M) for 24 h.

by SRC is involved in the regulation of autophagy.<sup>33,34</sup> Moreover, AMPK-mediated autophagy plays a role in cisplatin-induced chemoresistance.<sup>35</sup>

Following cisplatin treatment, the levels of phosphorylated SRC and phosphorylated AMPK were increased with cisplatin-induced GFRA1 expression in MG-63 cells, and the levels of

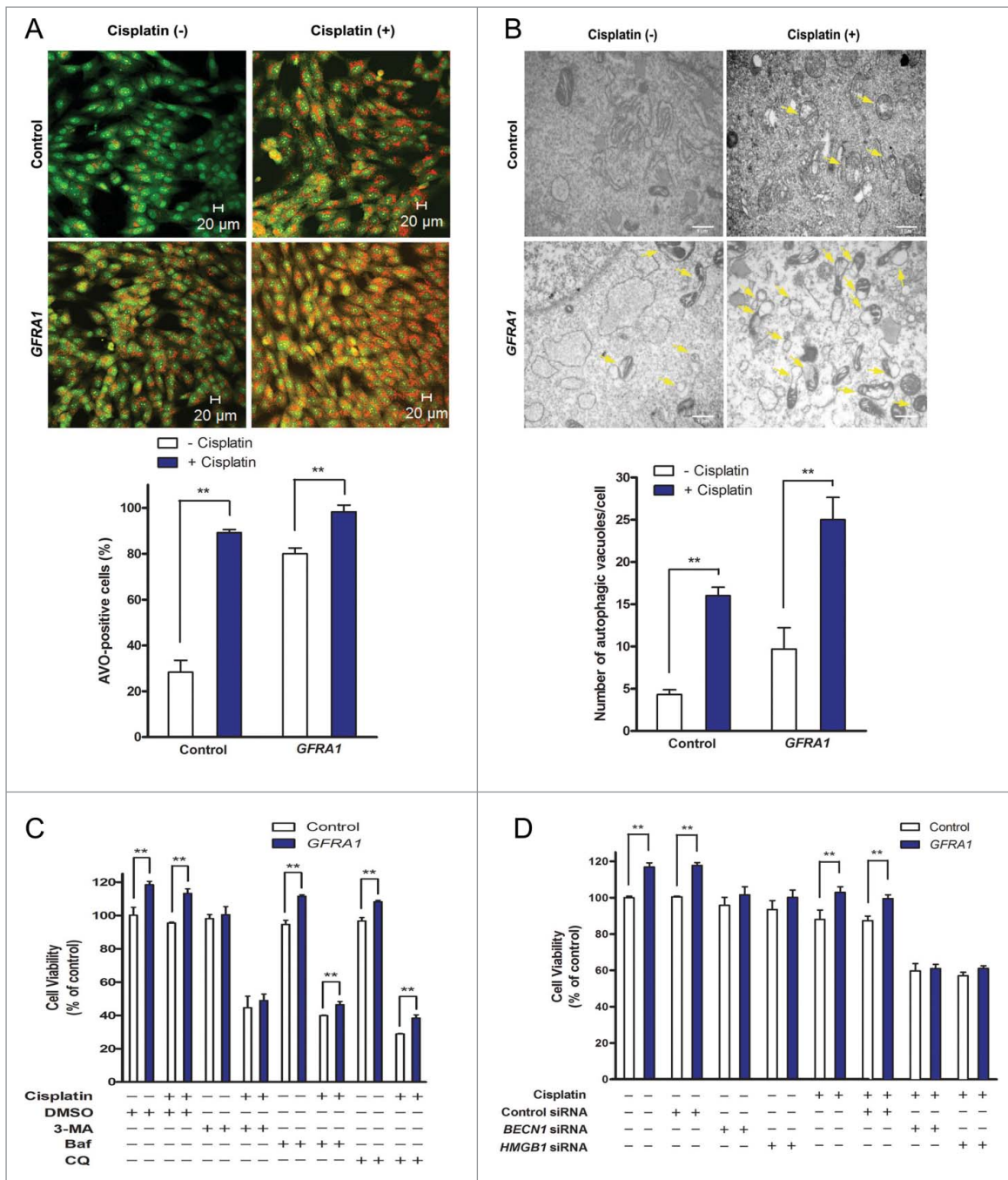


**Figure 5.** GFRA1-induced autophagy enhances the chemoresistance of osteosarcoma cells induced by cisplatin. (A) Control and GFRA1-overexpressing MG-63 cells were treated with cisplatin (20  $\mu$ M) for 24 h and then stained with acridine orange. Top, representative images of cells stained with acridine orange. Scale bar: 20  $\mu$ m. Bottom, quantitative analysis of the number of AVOs. (B) Control and GFRA1-overexpressing MG-63 cells were treated with cisplatin (20  $\mu$ M) for 24 h and then analyzed by TEM. Top, representative images of autophagic vacuoles detected after cisplatin treatment in control and GFRA1-overexpressing MG-63 cells. Scale bar: 100 nm. Bottom, quantitative analysis of the number of autophagic vacuoles. (C) Cell viability of GFRA1-overexpressing osteosarcoma cells after cisplatin treatment in the presence of autophagy inhibitors. Control or GFRA1-overexpressing MG-63 cells were cultured with DMSO, 3-MA (10 mM), Baf (100 nM), or CQ (30  $\mu$ g/ml), and then treated with cisplatin (20  $\mu$ M) for 24 h. Cell viability was measured using the WST-1 assay. (D) Cell viability of GFRA1-overexpressing osteosarcoma cells after cisplatin treatment in the presence of *BECN1* (20 nM) or *HMGB1* (20 nM) siRNA. Control or GFRA1-overexpressing MG-63 cells were cultured with *BECN1* or *HMGB1* siRNA for 48 h and then treated with cisplatin (20  $\mu$ M) for 24 h. Cell viability was measured using the WST-1 assay. The values are presented as a mean  $\pm$  s.d.m. (n = 3). \*\*denotes  $P < 0.05$ .

phosphorylated MTOR (mechanistic target of rapamycin [serine/threonine kinase]) and phosphorylated RPS6KB1/S6K/p70 S6Kinase, downstream kinases involved in AMPK signaling, were subsequently decreased (Fig. 8A). Upregulation of SRC-AMPK signaling by GFRA1 increased the expressions of *BECN1*, *HMGB1*, and production of LC3-II (Fig. 8A). In contrast, the levels of phosphorylated SRC and phosphorylated

AMPK were decreased and the levels of phosphorylated MTOR and phosphorylated RPS6KB1 were increased in GFRA1-deficient cells compared to control cells. Expression levels of autophagy-related proteins were then reduced in GFRA1-deficient cells compared to control cells (Fig. 8B). The polyubiquitin-binding protein SQSTM1/p62 (sequestosome 1) interacts and forms a complex with LC3 to signal for the targeted degradation



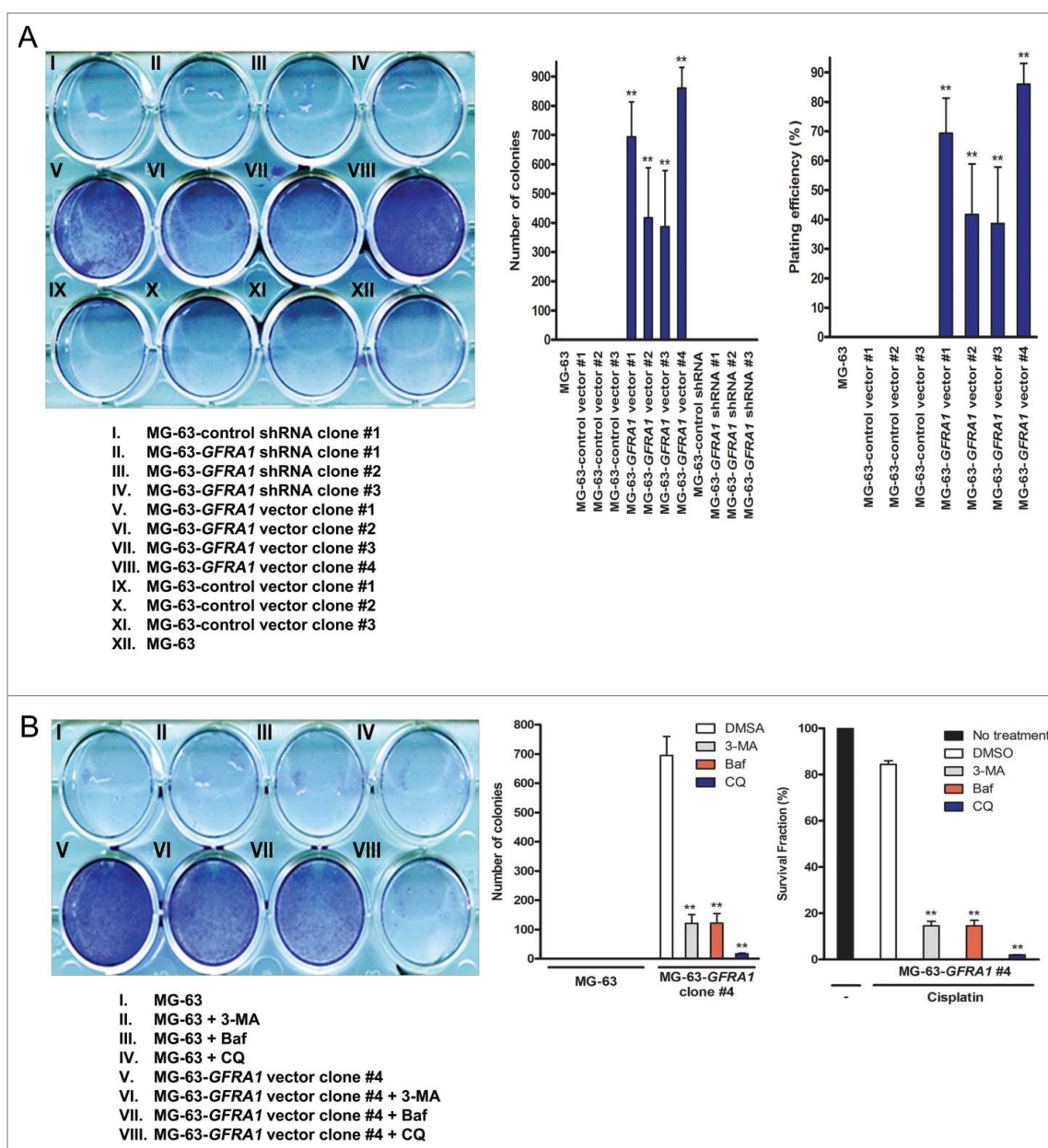


**Figure 6.** Overexpression of GFRA1 increases colony formation in the presence of cisplatin. (A) The effect of GFRA1 deficiency or overexpression on colony formation in the presence of cisplatin ( $20 \mu\text{M}$ ). Equal number ( $1 \times 10^4$  cells) of control (control shRNA), GFRA1-deficient (*GFRA1* shRNA), control (empty vector), and GFRA1-overexpressing (*GFRA1* expressing vector) MG-63 cells were plated. All of cell lines were incubated with cisplatin ( $20 \mu\text{M}$ ) for 10 d. Colonies were stained by crystal violet for visualization. Left, representative images of colony formation. Right, quantitative analysis of the number of colonies and plating efficiency. (B) The effect of autophagy inhibitors on the colony formation of GFRA1-overexpressing cells in the presence of cisplatin ( $20 \mu\text{M}$ ). Control and GFRA1-overexpressing clone #4 (See above Figure 3J) were plated and treated with 3-MA (10 mM), Baf (100 nM), or CQ ( $30 \mu\text{g/ml}$ ), respectively. All of cell lines were incubated with cisplatin for 10 d. All of the plates were scanned by a scanner and numbers of colonies were quantified by using imageJ software. Left, representative images of colony formation. Right, quantitative analysis of the number of colonies and survival fraction. The values are presented as a mean  $\pm$  s.d.m. ( $n = 3$ ). \*\*denotes  $P < 0.05$ .

of SQSTM1-associated polyubiquitin-containing inclusion bodies by autophagy.<sup>36,37</sup> However, recent studies showed that cisplatin-resistant ovarian cancer cells express much higher levels of SQSTM1 than do cisplatin-sensitive ovarian cancer cells.<sup>38,39</sup> In addition, the level of SQSTM1 was increased in osteosarcoma cell lines after cisplatin treatment following a temporary decrease at the onset of treatment.<sup>40</sup> Consistent with these studies, the level of SQSTM1 was increased in cisplatin-treated MG-63 cells (Fig. 8A) and decreased in GFRA1-deficient cells compared to control cells (Fig. 8B). It suggests that SQSTM1 is involved in a cisplatin-resistant mechanism by other signaling pathways rather than autophagy. Inhibition of SRC phosphorylation by either siRNA or

its selective inhibitor PP1 led to decreased AMPK phosphorylation and LC3-II production (Fig. 8C, D). Inhibition of AMPK phosphorylation by its selective inhibitor compound C also led to decreased LC3-II production with no effect on SRC phosphorylation (Fig. 8E), confirming that AMPK is a downstream kinase of SRC. Inhibition of either AMPK or SRC activation by their selective inhibitors in MG-63 cells significantly reduced cell viability after cisplatin treatment compared to controls (Fig. 8F, G, respectively). The data implies that following cisplatin treatment, induction of GFRA1 triggers SRC activation, which in turn activates AMPK signaling, leading to initiation of autophagy in osteosarcoma.

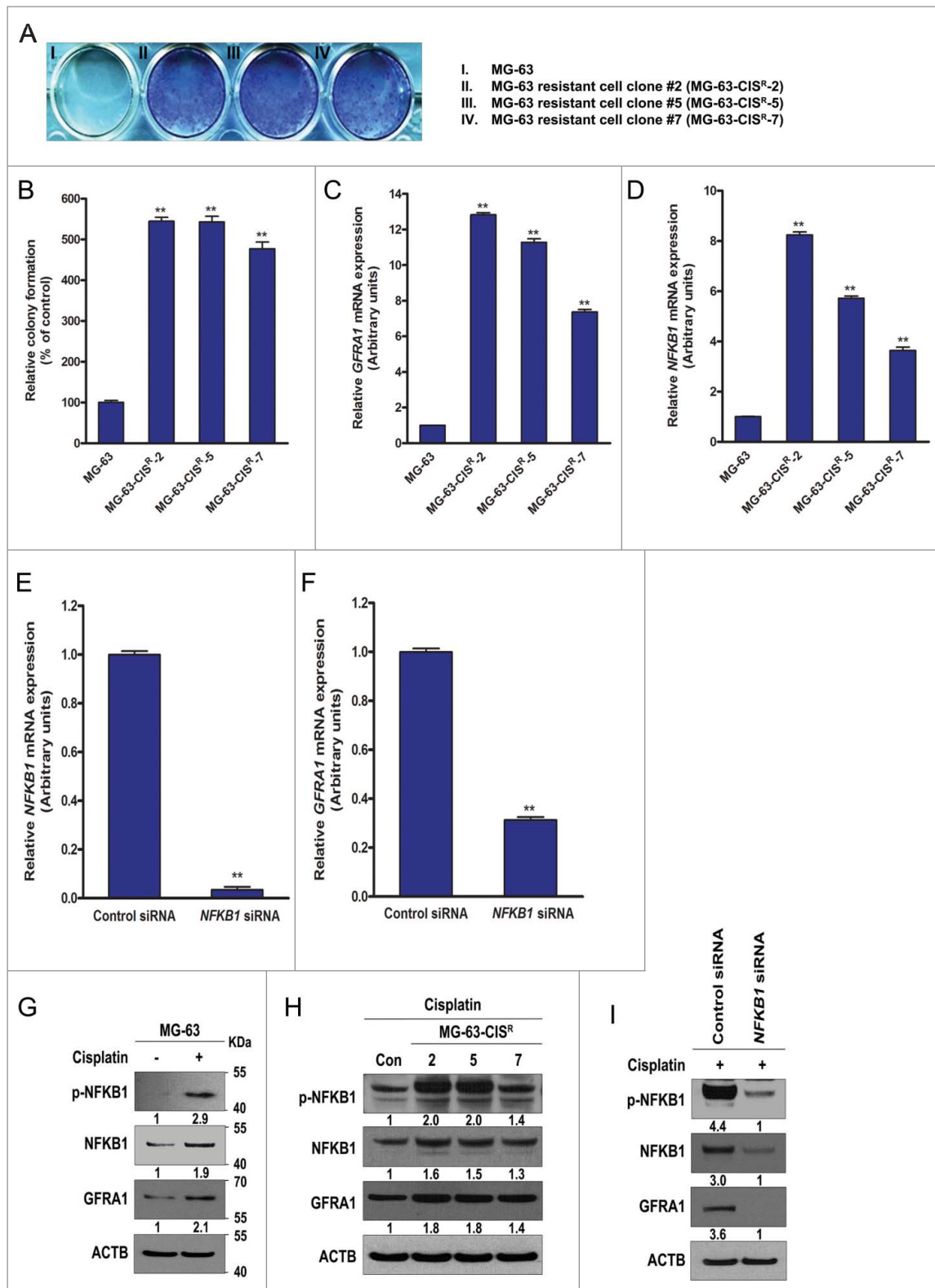


**Figure 7.** GFRA1 and NFKB1 expression in cisplatin-resistant MG-63 cells. (A) Representative images of colony formation in MG-63 resistant cell clones after cisplatin treatment for 10 d. (B) Quantitative analysis of the number of colonies. (C) Quantitative real-time PCR of GFRA1 mRNA expression in MG-63 (control) or MG-63 resistant cell clones 24 h after cisplatin treatment. (D) Quantitative real-time PCR of *NFKB1* mRNA expression in MG-63 (control) or MG-63 resistant cell clones 24 h after cisplatin treatment. (E) Quantitative real-time PCR of *NFKB1* mRNA expression in MG-63 cells transiently transfected with either control siRNA or *NFKB1* siRNA for 48 h and then treated with cisplatin for 24 h. (F) Quantitative real-time PCR of *GFRA1* mRNA expression in MG-63 cells transiently transfected with either control siRNA or *NFKB1* siRNA for 48 h and then treated with cisplatin for 24 h. The values are presented as a mean  $\pm$  s.d.m. ( $n = 3$ ). \*\*denotes  $P < 0.05$ . (G to I) Immunoblot analysis of osteosarcoma cell lysates with antibodies specific for GFRA1, p-NFKB1, NFKB1, and ACTB. (G) MG-63 cells were treated with cisplatin ( $20 \mu\text{M}$ ) for 24 h. (H) MG-63 (control) or MG-63 resistant cell clones were treated with cisplatin. (I) MG-63 resistant (MG-63-CIS<sup>R</sup>-2) cells were transiently transfected with either control siRNA or *NFKB1* siRNA (20 nM) for 48 h and then treated with cisplatin for 24 h.

### GFRA1-induced autophagy promotes tumor growth in vivo

GFRA1 is known to be a co-receptor of RET which is a proto-oncogene involved in tumor progression;<sup>41</sup> however, our study revealed RET expression is not detected in osteosarcoma after cisplatin treatment. Therefore, we examined the oncogenicity of GFRA1. NIH3T3 mouse fibroblast cells revealed that transfection with *GFRA1* expression vector induced cellular transformation, as shown by focus formation. NIH3T3 cells transfected with a control vector did not induce transformation (Fig. S7). The results imply GFRA1 has oncogenic capabilities and could promote tumor formation and consequently chemoresistance.

We next evaluated the effects of GFRA1 on tumor formation in vivo using mouse xenograft models. First, MG-63 control cells or GFRA1-overexpressing MG-63 cells (MG-63-*GFRA1*) were implanted subcutaneously in the right flank of nude mice. At 5 d after injection, mice injected with MG-63-*GFRA1* cells started to develop tumors and then after 31 d they produced large-sized tumors (~90 mm<sup>3</sup>) (Fig. 9A). However, mice injected with MG-63 control cells did not develop tumors until 17 d after injection and the resultant tumors were small (~10 mm<sup>3</sup>) (Fig. 9A). We examined the effect of GFRA1 deficiency on tumor formation by implanting GFRA1-deficient MG-63 cells (MG-63-*GFRA1* shRNA). Whereas mice injected with MG-63 control cells developed tumors, injection of MG-63-*GFRA1* shRNA cells into mice did not produce tumors even after 31 d (Fig. 9B).

Then, we assessed whether enhanced tumor formation observed in MG-63-*GFRA1* grafted mice resulted from GFRA1-mediated autophagy. Chloroquine is one of the leading agents that have been used in many recent clinical trials.<sup>42</sup> Therefore, we selected chloroquine to investigate the effect of autophagy inhibition in our in vivo models. After 31 d, tumor-bearing mice injected with MG-63-*GFRA1* cells were treated with PBS (control), CQ, cisplatin, or cisplatin + CQ. Treatment with either CQ or cisplatin decreased tumor volume compared to PBS-treated mice, and treatment of mice with both cisplatin and CQ significantly decreased tumor volume further (Fig. 9C). The results demonstrated that only treatment with both cisplatin and CQ reduced tumor progression while single treatment with either CQ or cisplatin allowed the tumors to survive (Fig. 9C). Immunofluorescence analysis revealed that tumor cells arising from MG-63-*GFRA1* grafted mice treated with cisplatin showed a significant increase in HMGB1 expression localized in the cytoplasm, signifying increased autophagy. Cotreatment of cisplatin with CQ significantly reduced cytoplasmic localization of HMGB1 (Fig. 9D and Fig. S8). Inhibition of autophagy with CQ during cisplatin treatment also significantly increased cisplatin-induced apoptosis in GFRA1-expressing tumors in comparison to CQ- or cisplatin-treated GFRA1-expressing tumors (Fig. 9E).

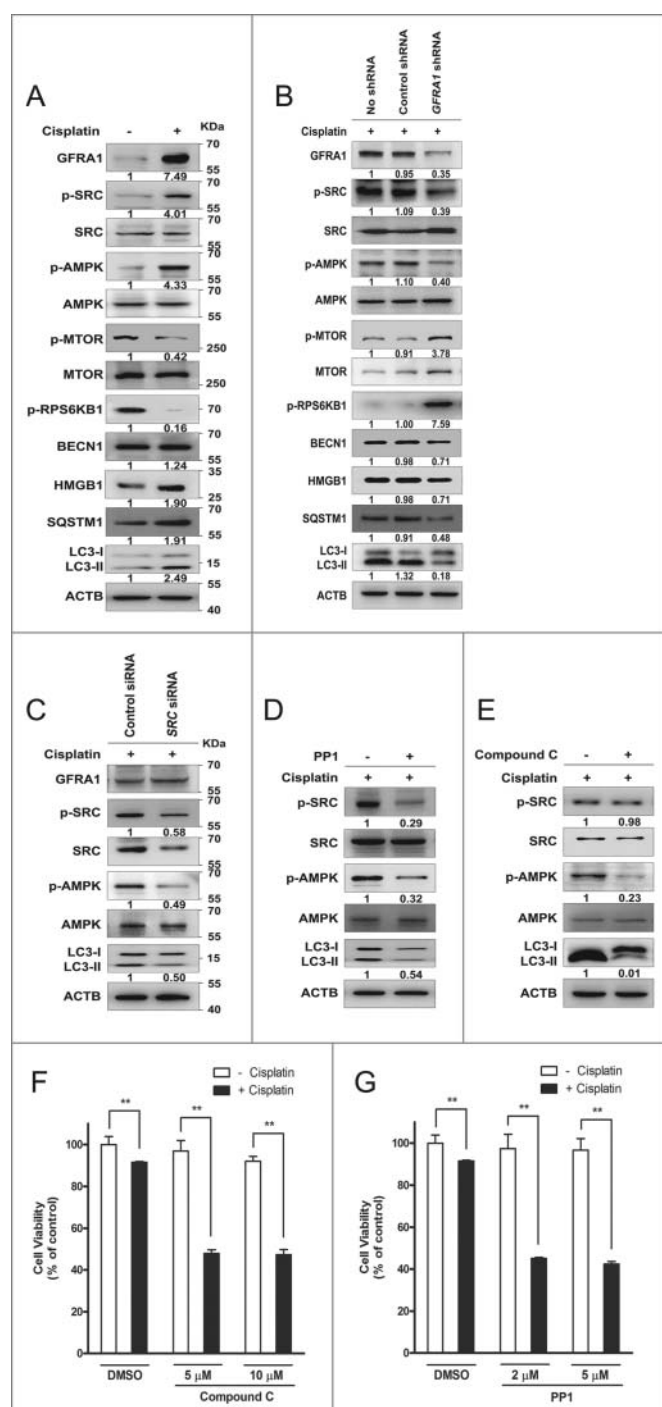


**Figure 8.** GFRA1 regulates autophagy by SRC-AMPK signaling in osteosarcoma cells. (A-B) Immunoblot analysis of osteosarcoma cell lysates with antibodies specific for GFRA1, p-SRC, SRC, p-AMPK, AMPK, p-MTOR, MTOR, p-RPS6KB1, BECN1, HMGB1, LC3, and ACTB. Immunoblots of ACTB expression shown are only representative. (A) MG-63 cells were treated with cisplatin (20 μM) for 24 h. The numbers below the lanes indicate densitometric quantification of the expression of the corresponding protein relative to ACTB control. The numbers below LC3 lane indicate the ratio of LC3-II to LC3-I. (B) Control and GFRA1-deficient MG-63 cells were treated with cisplatin (20 μM) for 24 h. The numbers below the lanes indicate densitometric quantification of the expression of the corresponding protein relative to ACTB control. The numbers below the LC3 lane indicate the ratio of LC3-II to LC3-I. (C to E) Immunoblot analysis of osteosarcoma cell lysates with antibodies specific for GFRA1, p-SRC, SRC, p-AMPK, AMPK, LC3, and ACTB. The numbers below the lanes indicate densitometric quantification of the expression of the corresponding protein relative to ACTB control. The numbers below LC3 lane indicate the ratio of LC3-II to LC3-I. (F) Cell viability of MG-63 cells after cisplatin treatment in the presence of PP1. MG-63 cells were cultured with DMSO or PP1 (2, 5 μM) and then treated with cisplatin (20 μM) for 24 h. Cell viability was measured using the WST-1 assay. (G) Cell viability of MG-63 cells after cisplatin treatment in the presence of compound C. MG-63 cells were cultured with DMSO or compound C (5, 10 μM) and then treated with cisplatin (20 μM) for 24 h. Cell viability was measured using the WST-1 assay. The values are presented as a mean ± s.d.m. (n = 3). \*\* denotes  $P < 0.05$ .

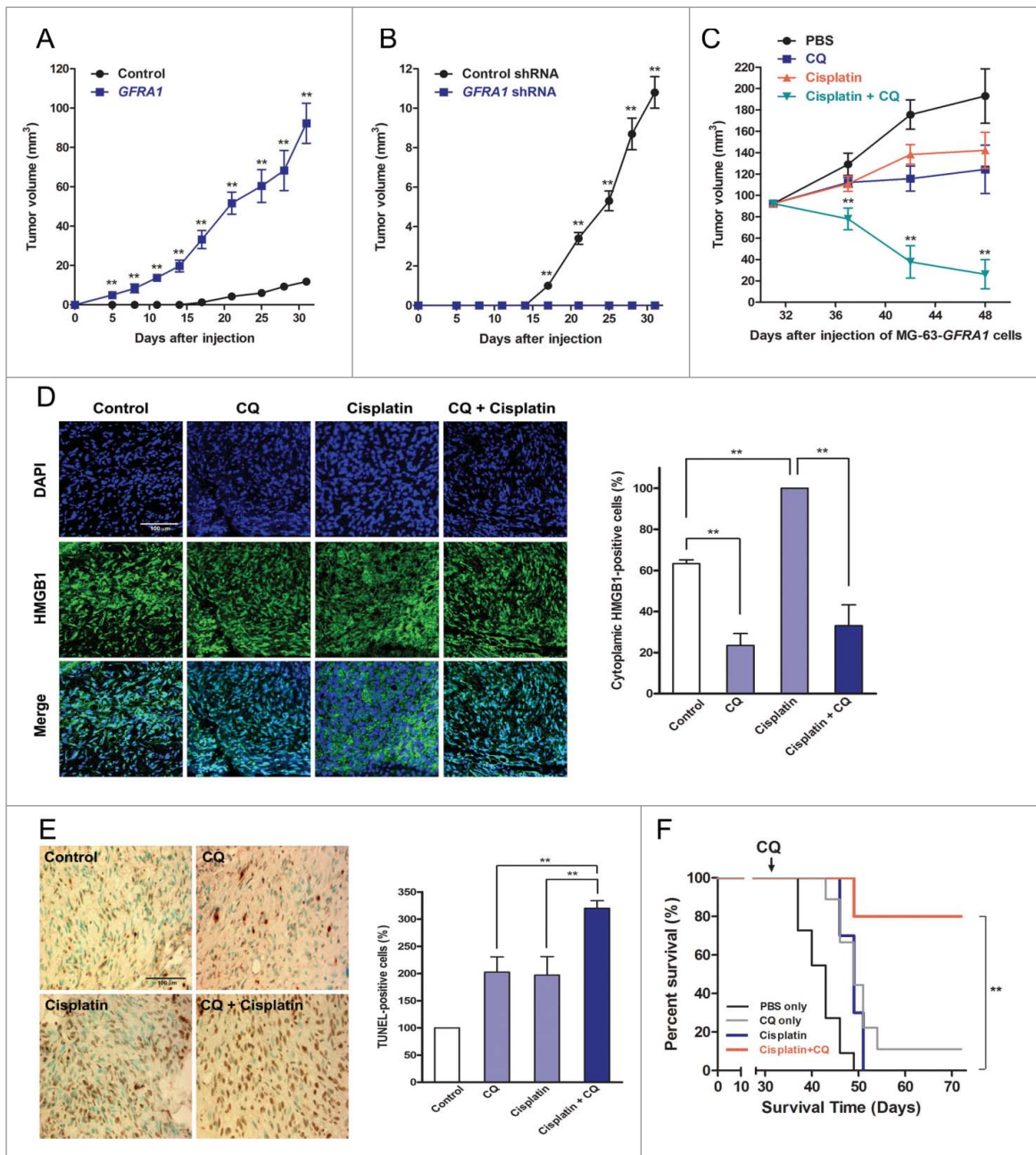


**Figure 9.** GFRA1-mediated autophagy promotes chemoresistance and tumor growth in vivo. (A) BALB/c nude mice ( $n = 80$ ) were injected with MG-63 cells that were transfected with either control or GFRA1-expressing vector. Tumor volume was measured every 3 or 4 d. (B) BALB/c nude mice ( $n = 20$ ) were injected with MG-63 cells that were transfected with either control or *GFRA1* shRNA. Tumor volume was measured every 3 or 4 d. Data are shown as mean  $\pm$  SEM.  $^{**}P < 0.05$ . (C) Tumors that were generated from mice injected with MG-63 cells containing *GFRA1*-expressing vector were directly injected with PBS, CQ, cisplatin, or cisplatin + CQ. Tumor volume was measured every 4 d. Data are shown as mean  $\pm$  SEM.  $^{**}P < 0.05$  vs PBS, CQ, or cisplatin-treated tumors. (D) Left, representative images of immunofluorescence staining of HMGB1 in a section from tumors generated from mice injected with MG-63 cells containing *GFRA1* expressing vector and then treated with PBS, CQ, cisplatin, or cisplatin + CQ. Scale bar: 100  $\mu$ m. Right, quantitative analysis of percentage of cytoplasmic HMGB1-positive cells in HMGB1-positive tumors. (E) Left, representative images of TUNEL-positive cells in a section from tumors generated from mice injected with MG-63 cells containing *GFRA1*-expressing vector and then treated with PBS, CQ, cisplatin, or cisplatin + CQ. Right, quantitative analysis of percentage of TUNEL-positive cells in HMGB1-positive tumors. The values are represented as a mean  $\pm$  s.d. m. ( $n = 3$ ).  $^{**}P < 0.05$ . Scale bar: 100  $\mu$ m. (F) Survival rate of mice injected with MG-63 cells containing *GFRA1*-expressing vector and then treated with PBS, CQ, cisplatin, or cisplatin + CQ.

Furthermore, the survival rate of MG-63-*GFRA1* grafted mice treated with both CQ and cisplatin was significantly increased compared to mice treated only with cisplatin (Fig. 9F), indicating that inhibition of autophagy reverses GFRA1-mediated protection from cisplatin-induced apoptosis. We note that, among 10 MG-63-*GFRA1* grafted mice treated with both CQ and cisplatin, 2 mice died due to cisplatin-induced liver and kidney injury, not due to

tumor at d 73, indicating the potential side effects in the combined use of CQ and cisplatin as previously reported.<sup>42</sup> Taken together, these results demonstrate that GFRA1 facilitates autophagy in response to cisplatin in vivo and this autophagic response promotes the survival of osteosarcoma tumors, suggesting that GFRA1-mediated autophagy is critical to the development of cisplatin resistance in osteosarcoma.

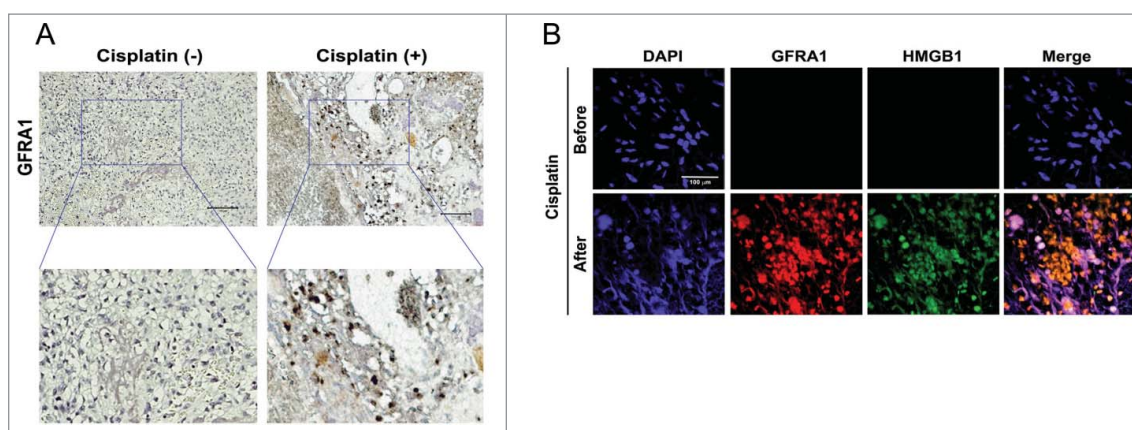


**Figure 10.** GFRA1 and HMGB1 expression in human osteosarcoma patient. (A) Representative images of immunohistochemical staining of GFRA1 in a section from human osteosarcoma patient before and after cisplatin treatment. Scale bar: 100  $\mu$ m. (B) Representative images of immunofluorescence staining of GFRA1 and HMGB1 in a section from human osteosarcoma patient before and after cisplatin treatment. Scale bar: 100  $\mu$ m.

### Contribution of GFRA1-mediated autophagy to clinicopathology of cisplatin-resistant osteosarcoma patients

We further investigated GFRA1-mediated autophagy *in vivo* by examining tissue samples from 27 osteosarcoma patients who had received neoadjuvant and adjuvant therapy along with complete surgical resection. Among those cases, 9 patient tissue samples displayed DAPI nuclear staining indicating survival of osteosarcoma (Table S1). HMGB1, especially cytosolic HMGB1, is an important marker in the regulation of autophagy. Studies also showed that HMGB1 is involved in chemotherapy resistance including cisplatin in leukemia and osteosarcoma cells.<sup>15,43</sup> From the 9 samples demonstrating chemoresistance, osteosarcoma tissues before and after cisplatin treatment were processed and analyzed for GFRA1 and HMGB1 immunostaining. Four samples were positive for GFRA1 expression and only these 4 GFRA1-positive samples were also positive for HMGB1 expression (Fig. 10A, B, Table 1, and Table S2). The 4 tissue samples were obtained from patients that received chemotherapy, including cisplatin, for 4 to 15 wk. Moreover, tumors from these 4 osteosarcoma patients metastasized to the lungs (Table 1 and Table S2). Tissue from patients that had been treated for less than 4 wk did not express GFRA1 and HMGB1 (Table 1 and Table S2). Collectively, these studies suggest a critical role for GFRA1 in cisplatin-mediated chemoresistance.

### Discussion

Chemoresistance arises in various ways mediated by drug export transporters, DNA repair mechanisms, cancer stem cells, resistance to apoptosis, self-sufficiency for growth factor signaling, angiogenic switch, and immunological pathways.<sup>16</sup> Autophagy can contribute to increased acquisition of chemoresistance in cancer; however, it also contributes to the inhibition of chemoresistance in some types of cancer.<sup>16,44</sup> These conflicting findings suggest that the role autophagy plays in chemoresistance may depend on the facilitating signaling mechanisms that are differentially regulated, based on cancer type and/or the chemotherapy strategy used. Therefore, elucidation of autophagic signaling mechanisms with regards to specific types of cancer and therapies is required to develop more effective chemotherapeutic combinations for cancer treatment. Our study provides the first evidence that the chemotherapy drug cisplatin induces expression of the GFRA1 receptor which inhibits cisplatin-mediated apoptosis and triggers autophagy for cell survival *in vitro* and *in vivo*, thereby promoting chemoresistance. We found tumors from 4 of 9 patients who had undergone extended cisplatin treatment expressed both GFRA1 and HMGB1 and metastasized to the lungs (Table 1 and Table S2). The clinical data substantiates the *in vivo* results seen in our xenograft mouse model, which implies similar results could have been obtained with an orthotopic model.

**Table 1.** Relative expression of GFRA1 and HMGB1, and metastatic status in osteosarcoma patients after combinational chemotherapy.

Case No	Tumor site	Combinational treatment	Treatment period (week)	GFRA1 expression	HMGB1 expression	Metastatic status
1	Distal femur	DOX, CIS	1	—	—	—
2	Distal femur	DOX, CIS	2	—	—	—
3	Fibular head	DOX, CIS	4	—	—	—
4	Distal femur	MTX, VCR, CIS	4	+	+	Lung
5	Mandible	DOX, CIS	5	—	—	—
6	Distal femur	IFO, DOX, CIS	8	+	+	Lung
7	Proximal femur	DOX, CIS	10	+	+	Lung
8	Distal femur	DOX, CIS	10	+	+	Lung
9	Distal femur	IFO, DOX, MTX, CIS	15	—	—	—

CIS, cisplatin; DOX, doxorubicin; IFO, ifosfamide; MTX, methotrexate; VCR, vincristine.

GFRA1 functions by binding to GDNF and when they are in complex GDNF-GFRA1 signaling can proceed through either activation of protooncogene SRC or through activation of RET which in turn activates SRC.<sup>20,21</sup> GDNF promotes resistance to the cytotoxic effects of all-*trans*-retinoic acid in neuroblastoma cells and it contributes to the chemoresistance to 1,3-bis(2-chloroethyl)-1-nitrosourea in glioblastoma cells by regulating survival signaling by AKT1/Akt (AKT serine/threonine kinase 1) and MAPK8/JNK1 (mitogen-activated protein kinase 8)-MAPK9/JNK2-MAPK10/JNK3.<sup>45,46</sup> GDNF significantly increases the survival of hair cells located in the cochlea of the inner ear after cisplatin treatment both in vivo and in vitro, indicating GDNF can be protective against cisplatin-induced ototoxicity.<sup>47,48</sup> Furthermore, GDNF is important to spermatogonial stem cell (SSC) proliferation and self-renewal by regulating transcription factors BCL6B, ERM, and LHX1 through SRC family kinase signaling.<sup>49</sup> In this regard, GDNF expression is increased along the basal Sertoli cell membrane, the physical location of the SSC niche, throughout the recovery period after repeated cisplatin treatment, indicating that redistribution of GDNF expression after cisplatin treatment is closely correlated with the expansion of the SSC population.<sup>50,51</sup>

GDNF did not have an effect on GFRA1-mediated cell survival and autophagy after cisplatin treatment (Fig. S2D, S2E), indicating that cisplatin-induced autophagy proceeds through GFRA1 signaling independently of GDNF. This data suggests that other ligands may be induced by cisplatin which bind GFRA1 to activate autophagy. Additionally, given that tyrosine kinases are important in cancer development, research has focused on the role of RET in GDNF signaling within cancer.<sup>52</sup> However, in our investigation, RET expression was not detected in either osteosarcoma or cisplatin-treated osteosarcoma cells (Fig. S6A).

In this study, we examined the effects of 3 chemotherapeutic agents (cisplatin, doxorubicin, and methotrexate) on GFRA1 expression.<sup>53</sup> Interestingly, only cisplatin increased the level of GFRA1 expression in osteosarcoma (Fig. 1A). Consistently, GFRA1 deficiency increased the sensitivity of osteosarcoma to cisplatin but not to the other 2 agents (Fig. S1). Previous studies showed that all 3 agents are able to induce HMGB1 expression and autophagy in osteosarcoma cells, which can increase chemoresistance<sup>43</sup>; therefore our current findings suggest that all 3 agents can contribute to chemoresistance in osteosarcoma through different autophagy signaling mechanisms.

APEX1 overexpression was observed in osteosarcoma patients treated with chemotherapy, suggesting its involvement in chemoresistance of osteosarcoma.<sup>54</sup> Previous work showed that APEX1 expression promoted pancreatic cancer progression by upregulating GFRA1 expression via activation of NFKB1.<sup>27</sup> Our current findings showed that APEX1 expression was not induced in osteosarcoma cells after cisplatin treatment (Fig. S6A). Similarly, knockdown of *APEX1* does not affect the level of LC3-II production or the accumulation of AVO-positive cells following cisplatin treatment (Fig. S6B, C). Interestingly, knockdown of *APEX1* in MG-63 cells increased the level of LC3-II production and AVO-positive cells compared to control cells without treatment (Fig. S6B, C), suggesting APEX1 has a function in autophagy unrelated to the GFRA1-SRC-AMPK mechanism induced by cisplatin. Additionally, our results revealed that NFKB1 plays a role in regulating GFRA1 expression in cisplatin-resistant MG-63 cell lines (Fig. 7A, B). The data suggest that cisplatin treatment induces GFRA1 expression through NFKB1 signaling independently of APEX1.

GFRA1 is expressed in several human cancers and it is involved in tumorigenesis through the regulation of migration and invasion. Therefore, it would be interesting to determine whether GFRA1 also has a role in the development of chemoresistance in other types of cancer, in addition to osteosarcoma. It

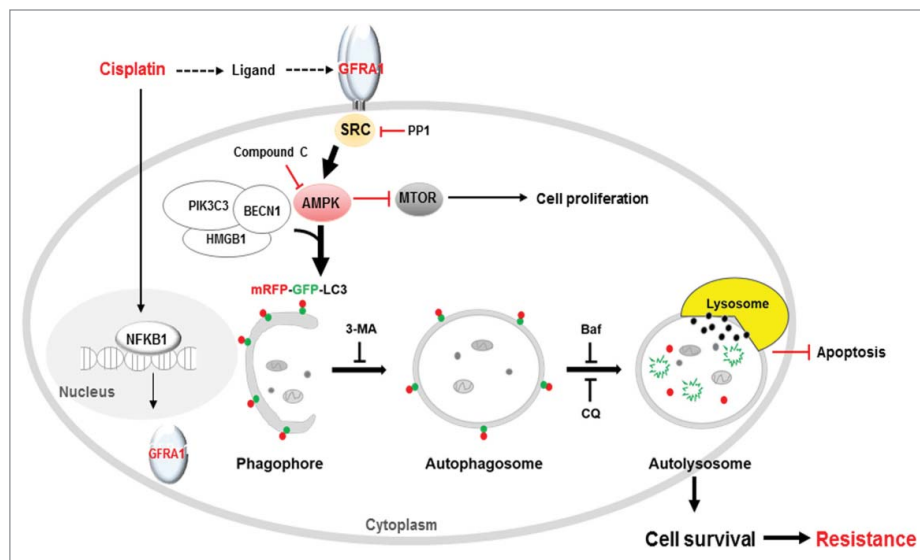


**Figure 11.** Schematic diagram for GFRA1-mediated autophagy in cisplatin-induced chemoresistance of osteosarcoma. Cisplatin treatment activates NFKB1 signaling in either a direct or indirect manner, subsequently activated NFKB1 can promote the expression of GFRA1 by binding the promoter region of the *GFRA1* gene.<sup>27</sup> Cisplatin may also induce other ligand(s) to bind and activate GFRA1. GFRA1 phosphorylates its downstream kinase SRC, which in turn activates AMPK-MTOR-dependent autophagy signaling. SRC inhibitor PP1 and AMPK inhibitor compound C can block cisplatin-induced autophagy. Inhibitors of autophagy, 3-MA, Baf, or CQ can also block cisplatin-induced autophagy. The regulation of GFRA1 expression and activation by cisplatin can contribute to the development of chemoresistance in osteosarcoma through SRC-AMPK-MTOR-mediated autophagy signaling, which is independent of GDNF, RET, or APEX1 signaling. 3-MA, 3-methyladenine; Baf, bafilomycin A1; CQ, chloroquine.

is also possible that other chemotherapeutic agents can induce GFRA1 expression to trigger autophagy in cancer cells, even though doxorubicin and methotrexate did not induce its expression in osteosarcoma cells. Interestingly, our results showed that the expression level of SQSTM1 was reduced in GFRA1-deficient cells after cisplatin treatment and increased in cells treated with cisplatin compared to control cells (Fig. 8A, B), implying SQSTM1 could be involved in a cisplatin-resistant mechanism facilitated by signaling pathways other than autophagy. Further work is needed to identify these alternative signaling pathways.

Taken together, our data showed that GFRA1 is a critical regulator in cisplatin-induced chemoresistance of osteosarcoma. Increased expression of GFRA1 by cisplatin, via NFKB1 signaling, induced the phosphorylation of its downstream kinase SRC and subsequently enhanced AMPK-MTOR-mediated autophagy, which contributes to chemoresistance (Fig. 11). This investigation suggests that GFRA1 could be a potential therapeutic target for the prevention of chemoresistance in osteosarcoma and possibly other types of cancers as well.

## Materials and methods

### Human tissue

Chonnam National University Hwasun Hospital (Gwangju, Chonnam, South Korea), a member of the National Biobank of Korea (<https://koreabiobank.re.kr>) supported by the Ministry of Health, Welfare, and Family Affairs, provided the biospecimens for this study. All specimens were obtained with informed consent under Chonnam National University School of Medicine Institutional Ethics Review Board-approved protocol.

### Cell culture

Human osteosarcoma cell lines MG-63 (ATCC, CRL-1427) and U-2 OS (ATCC, HTB-96), human embryonic kidney cell line 293T (ATCC, CRL-1573), human fibrosarcoma cell line HT-1080 (ATCC, CCL-121), human pancreatic cancer cell line MIA PaCa-2 (ATCC, CRL-1420), and mouse embryonic fibroblast cell line NIH/3T3 (ATCC, CRL-1658) were purchased from the American Type Culture Collection. Cell lines were maintained in Dulbecco modified Eagle medium (MG-63, 293T, MIA PaCa-2 and NIH/3T3), Eagle minimum essential medium (HT-1080) or McCoy 5a Modified Medium (U-2 OS) supplemented with 10% heat-inactivated fetal bovine serum (Gibco, 16000044) and 1% penicillin/streptomycin (10,000  $\mu\text{g}/\text{mL}/10,000\text{U}/\text{mL}$ , Gibco, 15140-122). Cells were maintained in 5%  $\text{CO}_2$ -humidified atmosphere at 37°C.

### Generation of stable cell lines

A human pLenti-GFRA1 expression vector (EX-Z4490-M02) and empty control vector (EX-NEG-M02) were purchased from GeneCopoeia. Viral packaging using 293T cells and titration of the full lentiviral vector were performed by using ViraPower™ Lentiviral Packaging Mix (Invitrogen, K497500). The presence of GFRA1 was confirmed by PCR, and correct insertion of the clone was further confirmed by sequencing.

Lentiviral transduction, expression, and titration were performed using HT-1080 cells. The packed virus was concentrated by Lenti-X Concentrator (Clontech, 631231). For establishing stable MG-63 and U-2 OS cell lines overexpressing GFRA1, cells were infected with lentivirus containing the pLenti-control or the pLenti-GFRA1 vector. Cells were then incubated in medium containing 400  $\mu\text{g}/\text{ml}$  of Geneticin/G-418 (Gibco, 10131027) for 4 to 5 wk. GFRA1-specific shRNA (sc-35469-SH) and control shRNA (sc-108060) were purchased from Santa Cruz Biotechnology. MG-63 and U-2 OS cells were transfected with either GFRA1-specific shRNA or control shRNA using Lipofectamine® 2000 (Invitrogen, 11668500) and cultured in selection medium containing 5  $\mu\text{g}/\text{ml}$  of puromycin (Gibco, A1113802) for 4 to 5 wk to generate stable GFRA1 knockdown cell lines. BECN1-specific shRNA (sc-29797-SH) was purchased from Santa Cruz Biotechnology to establish stable BECN1 knockdown MG-63 cell lines. For establishing NIH/3T3 cell lines overexpressing GFRA1, cells were transfected with GFRA1 expression vector and clones were selected with 400  $\mu\text{g}/\text{ml}$  of G-418 for 4 to 5 wk.

### Generation of cisplatin-resistant cell lines

Cisplatin-resistant (CIS<sup>R</sup>) sub-lines were derived from the MG-63 parental cell line by continuous exposure to cis-diamineplatinum(II) dichloride (cisplatin; Sigma-Aldrich, P4394) following initial dose-response studies of cisplatin (1  $\mu\text{M}$  to 1 mM) over 24 h from which IC50 values were obtained. Initially, the CIS<sup>R</sup> sub-line was treated with cisplatin (1  $\mu\text{M}$ ) for 72 h. The media was removed and cells were allowed to recover for 72 h. Subsequently, the resistant sub-lines were generated by gradual exposure to low to high-dosage of cisplatin (1 to 50  $\mu\text{M}$ ). This development period was carried out for approximately 6 mo, and then cells were maintained continuously in the presence of cisplatin at these new IC50 concentrations for 2 mo.

### Reagents and antibodies

Endotoxin-free GDNF (G1777) was purchased from Sigma-Aldrich and was reconstituted in filter-sterilized (0.2  $\mu\text{m}$ ) water. Dimethyl sulfoxide (DMSO) N, N-dimethylformamide, bafilomycin A<sub>1</sub> (Baf; 19-148), 3-methyladenine (3-MA; 189490) and chloroquine diphosphate salt (CQ; C6628) were purchased from Sigma-Aldrich. Cisplatin was dissolved in DMSO; accordingly, DMSO was used as a control vehicle for the experiments including cisplatin. Methotrexate (sc-3507) and doxorubicin (sc-280681) were purchased from Santa Cruz Biotechnology. The following antibodies were used: anti-GFRA1/GFR $\alpha$ -1 (sc-10716), anti-GFRA1 (sc-271546), anti-phospho-MTOR (sc-101738), anti-MTOR (sc-8319), anti-SRC/c-SRC (sc-8056), anti-CASP3/caspase-3 (sc-7148), anti-APEX1/APE1 (sc-17774), anti-ACTB/ $\beta$ -actin (sc-47778), anti-NFKB1/NF $\kappa$ B (sc-7178), and anti-phospho-NFKB1 (sc-271908) from Santa Cruz Biotechnology; anti-HMGB1 (ab18256) from Abcam; anti-phospho-SRC (Tyr416) (6943), anti-BECN1/Beclin 1 (3738), anti-phospho-AMPK (2535), anti-AMPK (2532), anti-LC3B (3868), anti-cleaved PARP (9548), and anti-phospho RPS6KB1/p70 S6 kinase/p-S6K (9205) from Cell Signaling Technology.

### Quantitative real-time (RT)-PCR (qPCR)

Total RNA was collected and isolated from cell lines using the RNeasy Mini Kit (Qiagen, 74104) according to the manufacturer's protocol. cDNA was generated from a 30- $\mu$ l reaction containing total RNA (3  $\mu$ g), reverse transcriptase (M1701), RNasin ribonuclease inhibitor (N2511), dNTP Mix (U1511) and oligo dT primers (C1101) purchased from Promega Corporation. Real-time amplification of *GFRA1* and *NFKB1* cDNA was performed with a LightCycler<sup>®</sup> 96 Instrument (Roche Diagnostics Corporation, Indianapolis, IN, USA) using SYBR<sup>®</sup> Mastermix FastStart Essential DNA Green Master (Roche). Gene-specific human primer pairs of 18S rRNA, *GFRA1* and *NFKB1* were designed using The Primer Express<sup>®</sup> software v3.0.1 (Applied Biosystems). The following primers were synthesized and used for qPCR: q18S rRNA sense primer 5'-GAGGATGAGGTG-GAACGTGT-3' and antisense primer 5'-TCTTCAGTCGCTC-CAGGCT-3' (designed to amplify a 166-bp region); q*GFRA1* sense primer 5'-TCCAATGTGTCGGGCAATAC-3' and antisense primer 5'-GGAGGAGCAGCCATTGATTT-3' (designed to amplify a 106-bp region); q*NFKB1* sense primer 5'-AAGCA-CAAAAAGGCAGCACT-3', antisense primer 5'-TGCCAAAT-GAGATGTTGTCGT-3' (designed to amplify a 197-bp region). The amplification conditions consisted of one cycle at 95°C for 10 sec followed by 48 cycles at 95°C for 5 sec and a 60°C annealing step for 20 sec. Amplification was followed by a melting curve analysis to verify the correct size of the amplicon. A negative control without cDNA was run with every PCR to assess the specificity of the reaction. An analysis of the data was performed using LightCycler<sup>®</sup> 96 software 1.1 (Roche Diagnostics International Ltd).

### Quantitative RT-PCR

Gene-specific human primer pairs of *GFRA1*, *GDNF* and *GAPDH* were designed using The Primer Express<sup>®</sup> software v3.0.1. The following primers were synthesized and used for PCR: *GFRA1* sense primer 5'-TGTCAGCAGCTGTCTAAAGG -3' and antisense primer 5'-CTTCTGTGCTGTAAATTTGCA-3' (designed to amplify a 387-bp region); *GDNF* sense primer 5'-CCAACCCA-GAGAATCCAGA-3' and antisense primer 5'-AGCCGCTG-CAGTACCTAAAA-3' (designed to amplify a 150-bp region); *GAPDH* sense primer 5'-TGACCACAGTCCATGCCATC-3' and antisense primer 5'-TTACTCCTTGAGGCCATGT-3' (designed to amplify a 494-bp region). PCR reactions were optimized to 94°C for 3 min, 28 amplification cycles at 94°C for 30 sec, 58°C for 30 sec, 72°C for 30 sec, and a final extension of 10 min at 72°C. Amplified products were resolved on 1.5% agarose gels and visualized by ethidium bromide staining.

### Small interfering RNA (siRNA)-based experiments

Human *GFRA1* siRNA (sc-35469), *BECN1* siRNA (sc-29797), *HMGB1* siRNA (sc-37982), *SRC/c-SRC* siRNA (sc-29228), *NFKB1* siRNA (sc-29407), *APEX1* siRNA (sc-29470) and negative (control) siRNA (sc-37007) were purchased from Santa Cruz Biotechnology. Cell lines were transiently transfected with siRNA duplexes using Lipofectamine<sup>™</sup> RNAiMAX (Life Technologies, 13778) according to the manufacturer's instructions.

### Cell viability assays

WST-1 cell viability assay (Roche Applied Science, 501003319) is based on the cleavage of a tetrazolium salt to form formazan in viable cells. Equal numbers of cells were seeded in triplicate wells in 48-well plates and maintained in growth medium containing 10% fetal bovine serum. Cells were cultured with DPBS (Gibco, 14190136), GDNF (50 ng/mL), GDNF (50 ng/ml) + cisplatin (20  $\mu$ M), or cisplatin (20  $\mu$ M) in the presence of serum for 24 h. Cells were also preincubated with inhibitors (3-MA, PP1, compound C, Baf and CQ) for 1 h before stimulating with DPBS, GDNF, GDNF + cisplatin, or cisplatin. WST-1 reagent was then treated to the cells at the indicated times and incubated for 2 h at 37°C. Cell viability was determined by measuring the absorbance after adding WST-1. The spectrophotometric absorbance of the samples was measured using an Ultra Multifunctional Microplate Reader (Tecan, Durham, NC, USA) at 450 nm. Experiments were done at least in triplicate using separate cultures.

### Apoptosis assays

Floating and trypsin-detached cells were collected and washed once with ice-cold PBS (Invitrogen, 003002), followed by FITC and ANXA5/Annexin V Apoptosis Detection Kit (BD Biosciences, BDB556547). Apoptotic cells were analyzed using a FACSCalibur flow cytometer with CellQuest software (Becton Dickinson, San Jose, CA, USA). The results represent the means of triplicate determinations in which a minimum of 10,000 cells was assayed for each determination. CASP3 activity was analyzed by the Colorimetric CaspACE<sup>™</sup> Assay System (Promega Corporation, G7351) according to the manufacturer's instructions. The degree of apoptosis in tissue was assessed with terminal deoxynucleotidyl transferase deoxyuridine triphosphate nick end labeling (TUNEL) assay from ApopTag<sup>®</sup> Plus Peroxidase In Situ Apoptosis Kit (EMD Millipore, S7101).

### FACS analysis

Cells were harvested by trypsinization, washed with phosphate-buffered saline (PBS), fixed in 70% ethanol, washed with PBS and then incubated with 0.02 mg/ml of propidium iodide including RNase A. Cells were analyzed using a FACSCalibur flow cytometer with CellQuest software.

### TUNEL assays

The apoptotic index in tissue was determined by the TUNEL assay. The sections were stained with ApopTag Plus Peroxidase In Situ Apoptosis Kit (EMD Millipore, S7101). The sections were incubated at 60°C overnight. Sections were deparaffinized in xylene for an hour and rehydrated with reduced alcohol series (100, 95, 90, 70, and 50%). The slides were incubated with 20  $\mu$ g/ml of proteinase K (Invitrogen, 4333793) for 15 min. Washing with PBS was performed in every stage. Endogenous peroxidase activity was blocked with 3% H<sub>2</sub>O<sub>2</sub>. After washing with PBS, the sections were incubated with equilibration buffer for 10 to 15 min, and with terminal deoxynucleotidyl transferase (TdT) enzyme (77  $\mu$ l reaction buffer +



33  $\mu$ l TdT enzyme mix [1  $\mu$ l TdT enzyme]) for 1 h at 37°C. Stop/wash buffer (1:10) was applied for 10 min at room temperature, and the slides were incubated with antidigoxigenin conjugate for 30 min. After washing with PBS 3 times for 5 min, the sections were stained with DAB components to detect TUNEL-positive cells, and then they were counterstained with methyl green. Data were quantified and analyzed with ImageJ software (National Institutes of Health).

### Autophagy assays

Formation of autophagic vesicles was monitored by endogenous or exogenous LC3-II aggregation in cell lines by LC3B antibody or *mRFP-GFP-LC3* plasmid provided by Dr. Myung Shik Lee from Samsung Medical Center, Sungkyunkwan University School of Medicine (Seoul, Korea). The protein levels of LC3-II in cells were determined by western blotting after treatment of cisplatin or autophagy inhibitors. Staining of acidic vesicular organelles (AVOs) by acridine orange (Polysciences, 04539-1) was performed according to published procedures.<sup>55</sup> Acridine orange was added at a final concentration of 0.5  $\mu$ g/ml for 15 min. All fluorescence images including AVOs and LC3 puncta in live cells (DAPI positive) are confocal images acquired with a LSM510 laser-scanning microscope (Carl Zeiss, Thornwood, NY, USA). Data were quantified and analyzed with ImageJ software. LC3-labeled puncta were defined as bright dots >1.5 SD above the mean cytosolic fluorescence. At least 3 individual experiments were performed, and at least 40 (for AVOs) or 20 (for LC3 puncta) sections were analyzed.<sup>15</sup>

### Transmission electron microscopy

Cells were fixed with 2% paraformaldehyde and 2% glutaraldehyde in 0.1 M phosphate buffer (pH 7.4) and then postfixed with 1% OsO<sub>4</sub> for 2 h. The cells were dehydrated with increasing concentrations of alcohol (30, 50, 70, 90, and 100%), infiltrated with LR White resin (Sigma, 62661) 2 times for 1 h, and embedded in LR White resin. The solidified blocks were cut into 60-nm thicknesses and stained with uranyl acetate and lead citrate. Samples were observed under a transmission electron microscope (Hitachi H-7600; Hitachi High-Technologies Corporation, Tokyo, Japan). Ten fields of images were selected and the autophagic vacuoles were quantified as previously described.<sup>56</sup>

### Colony-forming assays and crystal violet staining

MG-63 and MG-63 Resistant (MG-63-CIS<sup>R</sup>) cells, pLenti-*GFRA1*-, pLenti-empty vector-, sh*GFRA1*-, and control shRNA-transfected MG-63 cells were cultured in DMEM supplemented with 10% fetal bovine serum. For colony-formation assays, an equal numbers of cells from each individual clone were plated onto 12-well plates. After 24 h, cells were incubated with cisplatin, or cisplatin + autophagy inhibitors, respectively. All medium was exchanged every 3 d under the same condition. Colonies were visualized after 10 d. The cells were washed with PBS, fixed in 4% paraformaldehyde for 5 min, and again

washed with PBS. Fixed cells were stained with 0.05% crystal violet in distilled water for 1 h, washed with distilled water and then drained. Images of stained colonies were scanned using an Epson scanner (GT9700F; Tokyo, Japan) and then counted with Image-Pro Plus 5.1 software (Media Cybernetics). The experiments were repeated in triplicate.

### Focus-forming assays

NIH/3T3 cells ( $1 \times 10^6$ ) were plated onto 60-mm dishes and incubated overnight to form a monolayer. The next day, NIH/3T3 cells ( $1 \times 10^3$ ) stably transfected with an expression vector encoding *GFRA1* were plated on control NIH/3T3 cells. Medium was exchanged every 2 d and the foci was quantitated after 7 to 10 d. Cells stably transfected with the empty expression vector provide the negative control for this assay. All of the cells were stained with crystal violet (0.5% in 20% ethanol) for foci.

### Immunoblot analysis

Cells were washed with PBS and lysed in RIPA Buffer (Thermo Scientific, PI89900). The protein content was determined using a Bradford Protein Assay kit I (Bio-Rad, 5000001), and 10 to 50  $\mu$ g protein per lane was electrophoresed on 4–12% SDS polyacrylamide gels. Proteins were blotted onto Hybond ECL membranes (GE Healthcare Life Sciences, RPN303D). Two protein ladders were used for molecular weight determination. The blotted proteins were detected using an enhanced chemiluminescence detection system (iNtRON Biotechnology, 16024). Data were quantified and analyzed with ImageJ software.

### Immunocytochemistry

Osteosarcoma cells ( $2 \times 10^4$ ) were seeded on 60- $\mu$ m dishes 35 mm high (ibidi, GmbH). The following day, cells were fixed in 4% paraformaldehyde for 20 min. After being washed with PBS, and then incubated in 0.04% of Triton X-100 (MP Biomedicals, 04807423). After being washed again with PBS, they were incubated in 0.03% of BSA (Thermo Scientific, BP9706100) for 10 min at room temperature. Then, antibodies were applied overnight at 4°C and washed for 1 h in PBS. Alexa Fluor 488- or 647-conjugated secondary antibodies (Invitrogen, A-21121, A-21206, A-21236, and A-21245) were applied 1 h at 4°C and washed for 1 h in PBS. Slides were rinsed in PBS, mounted in VECTASHIELD Mounting Medium for Fluorescence with DAPI (Vector Laboratories, H-1200) and sealed with clear nail varnish. Images were taken by confocal microscopy. LC3 puncta was quantified and analyzed with ImageJ. In the above analysis, there was no discrepancy between the 2 observers regarding the patterns of biomarker expression and the scores assigned to analyzed sections.

### Immunohistochemistry

Triplicate core biopsies of viable tumor (1 mm) identified by 2 clinical pathologists were taken from each donor paraffin block and arrayed. The sections (5- $\mu$ m thick) were deparaffinized and underwent hematoxylin and eosin stain, and

immunohistochemistry. After antigen retrieval by 10 mM sodium citrate (pH 6.0), sections were incubated with rabbit anti-HMGB1 and mouse anti-GFRA1 antibodies for 24 h at 4°C. Sections were followed by incubation with biotinylated secondary antibodies, and then antibody labeling was visualized by using the VECTASTAIN ABC Systems (Vector Laboratories, PK6200). For immunofluorescence and immunohistochemistry, patient tissues and mouse tumors were incubated with the Alexa Fluor 488- and 647-conjugated secondary antibodies (Invitrogen, A-21121, A-21206, A-21236 and A-21245), and nuclei were counterstained with DAPI (Sigma-Aldrich, D9542). Then, one drop of ProLong Diamond Antifade 5 (Life Technologies, P36961) was directly applied to fluorescently labeled tissue samples on microscope slides. Immunofluorescence was detected by confocal microscopy. In patient tissue studies, immunoreactivity was not determined by scoring according to the staining intensity (0, non; 1, weak; 2, moderate; 3, strong) of immunolabeling and percent positive cells (0, <5%; 1, 6 to 25%; 2, 26 to 50%; 3, 51 to 75%; 4, 76% to 100%) because all of metastatic patient tissues between 4 and 10 wk after chemotherapy including cisplatin showed the robust immunoreactivity of GFRA1 or HMGB1, while other patient tissues, less than 4 wk or more than 10 wk after chemotherapy, with or without cisplatin never show the immunoreactivity of them. Thus, we marked plus (+) was considered to be positive immunoreactivity, while that minus (−) was considered to be negative immunoreactivity (not detected). In the above analysis, there was no discrepancy between the 2 observers regarding the patterns of biomarker expression and the scores assigned to analyzed sections. Data were quantified and analyzed with ImageJ software.

### Tumor formation in nude mice

The mice used in this study were 6-wk-old female BALB/c nude mice purchased from Orient Bio Inc. (Seongnam, South Korea). They were housed in our pathogen-free facility and handled in accordance with standard-use protocols and animal welfare regulations. All study protocols were approved by the institutional Animal Care and Use Committee at Chonnam National University. MG-63 cells stably transfected with the indicated Control shRNA, *GFRA1* shRNA, pLenti-*GFRA1* expression viral vector, or pLenti-control viral vector were harvested and resuspended in PBS. Then MG-63 cells ( $1 \times 10^6$ ) were injected subcutaneously into the right flank of a BALB/c nude mouse. The tumor size was measured with a caliper every 3 or 4 d. Thirty-one d after subcutaneous injection of MG-63-*GFRA1* cells, mice bearing tumors were administrated with PBS, CQ (60 mg/kg), cisplatin (3 mg/kg), and cisplatin + CQ into the peritoneum once a week. The tumor size was measured with a caliper every 4 d. Tumor weights were calculated from caliper measurements of tumor dimensions in mm using the formula for a prolate ellipsoid:  $(L \times W^2) / 2$  where L is the longer of the 2 measurements.

### Statistical analysis

Survival data was analyzed by the Kaplan–Meier and log-rank test with GraphPad Prism v5.04 (GraphPad Software). Plating

efficiency (PE, %) = (Number of colonies counted/Number of cells plated)  $\times$  100. Survival fraction (SF, %) = (PE of cisplatin-treated clone/ PE of nontreated control clone). All values are expressed as the mean  $\pm$  standard deviation (s.d.m.). Where indicated, we performed statistical analyses using a 2-tailed Student *t* test or ANOVA. \*\**P* < 0.05 was considered statistically significant.

### Abbreviations

3-MA	3-methyladenine
ACTB	actin, $\beta$
AMPK	AMP-activated protein kinase
ANXA5	annexin A5
APEX1	apurinic/apurimidinic endodeoxyribonuclease 1
AVO	acidic vesicular organelle
Baf	bafilomycin A1
BECN1	Beclin 1
CASP3	caspase 3
CIS	cisplatin
CIS <sup>R</sup>	cisplatin-resistant cell clone
CQ	chloroquine
DAPI	4',6-diamidino-2-phenylindole
DMSO	dimethyl sulfoxide
DOX	doxorubicin
FACS	fluorescence-activated cell sorting
FITC	fluorescein isothiocyanate
GAPDH	glyceraldehyde-3-phosphate dehydrogenase
GDNF	glial cell derived neurotrophic factor
GFP	green fluorescent protein
GFRA1	GDNF family receptor $\alpha$ 1
HMGB1	high mobility group box 1
IFO	ifosfamide
MAP1LC3/LC3	microtubule-associated protein 1 light chain 3
mRFP	monomeric red fluorescent protein
MTOR	mechanistic target of rapamycin (serine/threonine kinase)
MTX	methotrexate
NFKB1	nuclear factor kappa B subunit 1
PARP	poly(ADP-ribose) polymerase
PBS	phosphate-buffered saline
PCR	polymerase chain reaction
PP1	pyrazolopyrimidine compound 1
qPCR	quantitative real-time PCR
RPS6KB/p70S6K	ribosomal protein S6 kinase B
rRNA	ribosomal ribonucleic acid
shRNA	small hairpin RNA
siRNA	small interfering RNA
SQSTM1/p62	sequestosome 1
SSC	spermatogonial stem cell
TEM	transmission electron microscopy
TUNEL	terminal deoxynucleotidyl transferase dUTP nick end labeling
VCR	vincristine

## Disclosure of potential conflicts of interest

No potential conflicts of interest were disclosed.

## Acknowledgments

The biospecimens used for this study were provided by Korea Biobank Network, which is supported by the Ministry of Health, Welfare and Family Affairs. All samples derived from Korea Biobank Network were obtained with informed consent under institutional review board-approved protocols.

## Funding

This work was supported by the institutional fund from the Edinburgh Regional Academic Health Center, University of Texas Health Science Center at San Antonio and National Institutes of Health, NIEHS, Grant ES022250 (to D.J. Kim). This work was also supported by Basic research grant 2010-0004810 from National Research Foundation of Korea (to M. Kim). Also, this work was supported the National Research Foundation of Korea (NRF) grants funded by the Korea government MSIP, 2011-0030121 and 20141A2A2A01007582 (to W.J. Kim), and MSIP, 2015R1A2A2A01006595 (to J.-Y. Jung).

## References

- [1] Ottaviani G, Jaffe N. The epidemiology of osteosarcoma. *Cancer Treat Res* 2009; 152:3-13; PMID:20213383; [http://dx.doi.org/10.1007/978-1-4419-0284-9\\_1](http://dx.doi.org/10.1007/978-1-4419-0284-9_1)
- [2] Collins M, Wilhelm M, Conyers R, Herschtal A, Whelan J, Bielack S, Kager L, Kühne T, Sydes M, Gelderblom H, et al. Benefits and adverse events in younger versus older patients receiving neoadjuvant chemotherapy for osteosarcoma: findings from a meta-analysis. *J Clin Oncol* 2013; 31:2303-12; PMID:23669227; <http://dx.doi.org/10.1200/JCO.2012.43.8598>
- [3] Kansara M, Teng MW, Smyth MJ, Thomas DM. Translational biology of osteosarcoma. *Nat Rev Cancer* 2014; 14:722-35; PMID:25319867; <http://dx.doi.org/10.1038/nrc3838>
- [4] Meyers PA, Schwartz CL, Krailo M, Kleinerman ES, Betcher D, Bernstein ML, Conrad E, Ferguson W, Gebhardt M, Goorin AM, et al. Osteosarcoma: a randomized, prospective trial of the addition of ifosfamide and/or muramyl tripeptide to cisplatin, doxorubicin, and high-dose methotrexate. *J Clin Oncol* 2005; 23:2004-11; PMID:15774791; <http://dx.doi.org/10.1200/JCO.2005.06.031>
- [5] Dasari S, Tchounwou PB. Cisplatin in cancer therapy: molecular mechanisms of action. *Eur J Pharmacol* 2014; 740:364-78; PMID:25058905; <http://dx.doi.org/10.1016/j.ejphar.2014.07.025>
- [6] He H, Ni J, Huang J. Molecular mechanisms of chemoresistance in osteosarcoma (Review). *Oncol Lett* 2014; 7:1352-62; PMID:24765137
- [7] Lum JJ, DeBerardinis RJ, Thompson CB. Autophagy in metazoans: cell survival in the land of plenty. *Nat Rev Mol Cell Biol* 2005; 6:439-48; PMID:15928708; <http://dx.doi.org/10.1038/nrm1660>
- [8] Boya P, Reggiori F, Codogno P. Emerging regulation and functions of autophagy. *Nat Cell Biol* 2013; 15:713-20; PMID:23817233; <http://dx.doi.org/10.1038/ncb2788>
- [9] Levine B, Klionsky DJ. Development by self-digestion: molecular mechanisms and biological functions of autophagy. *Dev Cell* 2004; 6:463-77; PMID:15068787; [http://dx.doi.org/10.1016/S1534-5807\(04\)00099-1](http://dx.doi.org/10.1016/S1534-5807(04)00099-1)
- [10] Mizushima N. Autophagy: process and function. *Genes Dev* 2007; 21:2861-73; PMID:18006683; <http://dx.doi.org/10.1101/gad.1599207>
- [11] Kondo Y, Kanzawa T, Sawaya R, Kondo S. The role of autophagy in cancer development and response to therapy. *Nat Rev Cancer* 2005; 5:726-34; PMID:16148885; <http://dx.doi.org/10.1038/nrc1692>
- [12] Levine B. Unraveling the role of autophagy in cancer. *Autophagy* 2006; 2:65-6; PMID:16874090; <http://dx.doi.org/10.4161/auto.2.2.2457>
- [13] Mathew R, Karantza-Wadsworth V, White E. Role of autophagy in cancer. *Nat Rev Cancer* 2007; 7:961-7; PMID:17972889; <http://dx.doi.org/10.1038/nrc2254>
- [14] Chen N, Karantza-Wadsworth V. Role and regulation of autophagy in cancer. *Biochim Biophys Acta* 2009; 1793:1516-23; PMID:19167434; <http://dx.doi.org/10.1016/j.bbamcr.2008.12.013>
- [15] Liu L, Yang M, Kang R, Wang Z, Zhao Y, Yu Y, Xie M, Yin X, Livesey KM, Lotze MT, et al. HMGB1-induced autophagy promotes chemotherapy resistance in leukemia cells. *Leukemia* 2011; 25:23-31; PMID:20927132; <http://dx.doi.org/10.1038/leu.2010.225>
- [16] Sui X, Chen R, Wang Z, Huang Z, Kong N, Zhang M, Han W, Lou F, Yang J, Zhang Q, et al. Autophagy and chemotherapy resistance: a promising therapeutic target for cancer treatment. *Cell Death Dis* 2013; 4:e838; PMID:24113172; <http://dx.doi.org/10.1038/cddis.2013.350>
- [17] Ding ZB, Hui B, Shi YH, Zhou J, Peng YF, Gu CY, Yang H, Shi GM, Ke AW, Wang XY, et al. Autophagy activation in hepatocellular carcinoma contributes to the tolerance of oxaliplatin via reactive oxygen species modulation. *Clin Cancer Res* 2011; 17:6229-38; PMID:21825039; <http://dx.doi.org/10.1158/1078-0432.CCR-11-0816>
- [18] Liu L, Yang M, Kang R, Wang Z, Zhao Y, Yu Y, Xie M, Yin X, Livesey KM, Loze MT, et al. DAMP-mediated autophagy contributes to drug resistance. *Autophagy* 2011; 7:112-4; PMID:21068541; <http://dx.doi.org/10.4161/auto.7.1.14005>
- [19] Kang R, Tang D, Schapiro NE, Livesey KM, Farkas A, Loughran P, Bierhaus A, Lotze MT, Zeh HJ. The receptor for advanced glycation end products (RAGE) sustains autophagy and limits apoptosis, promoting pancreatic tumor cell survival. *Cell Death Differ* 2010; 17:666-76; PMID:19834494; <http://dx.doi.org/10.1038/cdd.2009.149>
- [20] Airaksinen MS, Saarma M. The GDNF family: signalling, biological functions and therapeutic value. *Nat Rev Neurosci* 2002; 3:383-94; PMID:11988777; <http://dx.doi.org/10.1038/nrn812>
- [21] Treanor JJ, Goodman L, de Sauvage F, Stone DM, Poulsen KT, Beck CD, Gray C, Armanini MP, Pollock RA, Hefti F, et al. Characterization of a multicomponent receptor for GDNF. *Nature* 1996; 382:80-3; PMID:8657309; <http://dx.doi.org/10.1038/382080a0>
- [22] Beshpalov MM, Saarma M. GDNF family receptor complexes are emerging drug targets. *Trends Pharmacol Sci* 2007; 28:68-74; PMID:17218019; <http://dx.doi.org/10.1016/j.tips.2006.12.005>
- [23] Paratcha G, Ledda F. GDNF and GFRalpha: a versatile molecular complex for developing neurons. *Trends Neurosci* 2008; 31:384-91; PMID:18597864; <http://dx.doi.org/10.1016/j.tins.2008.05.003>
- [24] Essegir S, Todd SK, Hunt T, Poulson R, Plaza-Menacho I, Reis-Filho JS, Isacke CM. A role for glial cell derived neurotrophic factor induced expression by inflammatory cytokines and RET/GFR alpha 1 receptor up-regulation in breast cancer. *Cancer Res* 2007; 67:11732-41; PMID:18089803; <http://dx.doi.org/10.1158/0008-5472.CAN-07-2343>
- [25] Wu ZS, Pandey V, Wu WY, Ye S, Zhu T, Lobie PE. Prognostic significance of the expression of GFRalpha1, GFRalpha3 and syndecan-3, proteins binding ARTEMIS, in mammary carcinoma. *BMC Cancer* 2013; 13:34; PMID:23351331; <http://dx.doi.org/10.1186/1471-2407-13-34>
- [26] Cavel O, Shomron O, Shabtay A, Vital J, Trejo-Leider L, Weizman N, Krelin Y, Fong Y, Wong RJ, Amit M, et al. Endoneurial macrophages induce perineural invasion of pancreatic cancer cells by secretion of GDNF and activation of RET tyrosine kinase receptor. *Cancer Res* 2012; 72:5733-43; PMID:22971345; <http://dx.doi.org/10.1158/0008-5472.CAN-12-0764>
- [27] Kim MH, Kim HB, Acharya S, Sohn HM, Jun JY, Chang IY, You HJ. Ape1/Ref-1 induces glial cell-derived neurotrophic factor (GDNF) responsiveness by upregulating GDNF receptor alpha1 expression. *Mol Cell Biol* 2009; 29:2264-77; PMID:19188437; <http://dx.doi.org/10.1128/MCB.01484-08>
- [28] Mizushima N, Yoshimori T, Levine B. Methods in mammalian autophagy research. *Cell* 2010; 140:313-26; PMID:20144757; <http://dx.doi.org/10.1016/j.cell.2010.01.028>
- [29] Kimura S, Noda T, Yoshimori T. Dissection of the autophagosome maturation process by a novel reporter protein, tandem fluorescent-

- tagged LC3. *Autophagy* 2007; 3:452-60; PMID:17534139; <http://dx.doi.org/10.4161/auto.4451>
- [30] Poteryaev D, Titievsky A, Sun YF, Thomas-Crusells J, Lindahl M, Billaud M, Arumäe U, Saarma M. GDNF triggers a novel Ret-independent Src kinase family-coupled signaling via a GPI-linked GDNF receptor alpha 1. *FEBS Letters* 1999; 463:63-6; PMID:10601639; [http://dx.doi.org/10.1016/S0014-5793\(99\)01590-2](http://dx.doi.org/10.1016/S0014-5793(99)01590-2)
- [31] Meley D, Bauvy C, Houben-Weerts JH, Dubbelhuis PF, Helmond MT, Codogno P, Meijer AJ. AMP-activated protein kinase and the regulation of autophagic proteolysis. *J Biol Chem* 2006; 281:34870-9; PMID:16990266; <http://dx.doi.org/10.1074/jbc.M605488200>
- [32] Ahn JH, Lee M. Suppression of autophagy sensitizes multidrug resistant cells towards Src tyrosine kinase specific inhibitor PP2. *Cancer Lett* 2011; 310:188-97; PMID:21775053; <http://dx.doi.org/10.1016/j.canlet.2011.06.034>
- [33] Zou MH, Hou XY, Shi CM, Kirkpatrick S, Liu F, Goldman MH, Cohen RA. Activation of 5'-AMP-activated kinase is mediated through c-Src and phosphoinositide 3-kinase activity during hypoxia-reoxygenation of bovine aortic endothelial cells. Role of peroxynitrite. *J Biol Chem* 2003; 278:34003-10; PMID:12824177; <http://dx.doi.org/10.1074/jbc.M300215200>
- [34] Mizrachi-Schwartz S, Cohen N, Klein S, Kravchenko-Balasha N, Levitzki A. Up-regulation of AMP-activated protein kinase in cancer cell lines is mediated through c-Src activation. *J Biol Chem* 2011; 286:15268-77; PMID:21245141; <http://dx.doi.org/10.1074/jbc.M110.211813>
- [35] Harhaji-Trajkovic L, Vilimanovich U, Kravic-Stevovic T, Bumbasir-ovic V, Trajkovic V. AMPK-mediated autophagy inhibits apoptosis in cisplatin-treated tumour cells. *J Cell Mol Med* 2009; 13:3644-54; PMID:20196784; <http://dx.doi.org/10.1111/j.1582-4934.2009.00663.x>
- [36] Pankiv S, Clausen TH, Lamark T, Brech A, Bruun JA, Outzen H, Øvervatn A, Bjørkøy G, Johansen T. p62/SQSTM1 binds directly to Atg8/LC3 to facilitate degradation of ubiquitinated protein aggregates by autophagy. *J Biol Chem* 2007; 282:24131-45; PMID:17580304; <http://dx.doi.org/10.1074/jbc.M702824200>
- [37] Ichimura Y, Kominami E, Tanaka K, Komatsu M. Selective turnover of p62/A170/SQSTM1 by autophagy. *Autophagy* 2008; 4:1063-6; PMID:18776737; <http://dx.doi.org/10.4161/auto.6826>
- [38] Yu H, Su J, Xu Y, Kang J, Li H, Zhang L, Yi H, Xiang X, Liu F, Sun L. p62/SQSTM1 involved in cisplatin resistance in human ovarian cancer cells by clearing ubiquitinated proteins. *Eur J Cancer* 2011; 47:1585-94; PMID:21371883; <http://dx.doi.org/10.1016/j.ejca.2011.01.019>
- [39] Xia M, Yu H, Gu S, Xu Y, Su J, Li H, Kang J, Cui M. p62/SQSTM1 is involved in cisplatin resistance in human ovarian cancer cells via the Keap1-Nrf2-ARE system. *Int J Oncol* 2014; 45:2341-8; PMID:25269472
- [40] Shen C, Wang W, Tao L, Liu B, Yang Z, Tao H. Chloroquine blocks the autophagic process in cisplatin-resistant osteosarcoma cells by regulating the expression of p62/SQSTM1. *Int J Mol Med* 2013; 32:448-56; PMID:23722646
- [41] Carlomagno F, Melillo RM, Visconti R, Salvatore G, De Vita G, Lupoli G, Yu Y, Jing S, Vecchio G, Fusco A, et al. Glial cell line-derived neurotrophic factor differentially stimulates ret mutants associated with the multiple endocrine neoplasia type 2 syndromes and Hirschsprung's disease. *Endocrinology* 1998; 139:3613-9; PMID:9681515
- [42] Kimura T, Takabatake Y, Takahashi A, Isaka Y. Chloroquine in cancer therapy: a double-edged sword of autophagy. *Cancer Res* 2013; 73:3-7; PMID:23288916; <http://dx.doi.org/10.1158/0008-5472.CAN-12-2464>
- [43] Huang J, Ni J, Liu K, Yu Y, Xie M, Kang R, Vernon P, Cao L, Tang D. HMGB1 promotes drug resistance in osteosarcoma. *Cancer Res* 2012; 72:230-8; PMID:22102692; <http://dx.doi.org/10.1158/0008-5472.CAN-11-2001>
- [44] Degenhardt K, Mathew R, Beaudoin B, Bray K, Anderson D, Chen G, Mukherjee C, Shi Y, Gélinas C, Fan Y, et al. Autophagy promotes tumor cell survival and restricts necrosis, inflammation, and tumorigenesis. *Cancer Cell* 2006; 10:51-64; PMID:16843265; <http://dx.doi.org/10.1016/j.ccr.2006.06.001>
- [45] Ng WH, Wan GQ, Peng ZN, Too HP. Glial cell-line derived neurotrophic factor (GDNF) family of ligands confer chemoresistance in a ligand-specific fashion in malignant gliomas. *J Clin Neurosci* 2009; 16:427-36; PMID:19138852; <http://dx.doi.org/10.1016/j.jocn.2008.06.002>
- [46] Hansford LM, Marshall GM. Glial cell line-derived neurotrophic factor (GDNF) family ligands reduce the sensitivity of neuroblastoma cells to pharmacologically induced cell death, growth arrest and differentiation. *Neurosci Lett* 2005; 389:77-82; PMID:16125842; <http://dx.doi.org/10.1016/j.neulet.2005.07.034>
- [47] Weissbluth S, Pitaro J, Daniel SJ. Gene therapy for cisplatin-induced ototoxicity: a systematic review of in vitro and experimental animal studies. *Otol Neurotol* 2012; 33:302-10; PMID:22388732; <http://dx.doi.org/10.1097/MAO.0b013e318248ee66>
- [48] Kuang R, Hever G, Zajic G, Yan Q, Collins F, Louis JC, Keithley E, Magal E. Glial cell line-derived neurotrophic factor. Potential for ototoxicity. *Ann N Y Acad Sci* 1999; 884:270-91; PMID:10842600; <http://dx.doi.org/10.1111/j.1749-6632.1999.tb08648.x>
- [49] Oatley JM, Avarbock MR, Brinster RL. Glial cell line-derived neurotrophic factor regulation of genes essential for self-renewal of mouse spermatogonial stem cells is dependent on Src family kinase signaling. *J Biol Chem* 2007; 282:25842-51; PMID:17597063; <http://dx.doi.org/10.1074/jbc.M703474200>
- [50] Harman JG, Richburg JH. Cisplatin-induced alterations in the functional spermatogonial stem cell pool and niche in C57/BL/6J mice following a clinically relevant multi-cycle exposure. *Toxicol Lett* 2014; 227:99-112; PMID:24704392; <http://dx.doi.org/10.1016/j.toxlet.2014.03.019>
- [51] Hofmann MC. Gdnf signaling pathways within the mammalian spermatogonial stem cell niche. *Mol Cell Endocrinol* 2008; 288:95-103; PMID:18485583; <http://dx.doi.org/10.1016/j.mce.2008.04.012>
- [52] Mulligan LM. RET revisited: expanding the oncogenic portfolio. *Nat Rev Cancer* 2014; 14:173-86; PMID:24561444; <http://dx.doi.org/10.1038/nrc3680>
- [53] Ferrari S, Ruggieri P, Cefalo G, Tamburini A, Capanna R, Fagioli F, Comandone A, Bertulli R, Bisogno G, Palmerini E, et al. Neoadjuvant chemotherapy with methotrexate, cisplatin, and doxorubicin with or without ifosfamide in nonmetastatic osteosarcoma of the extremity: an Italian sarcoma group trial ISG/OS-1. *J Clin Oncol* 2012; 30:2112-8; PMID:22564997; <http://dx.doi.org/10.1200/JCO.2011.38.4420>
- [54] Yang J, Yang D, Cogdell D, Du X, Li H, Pang Y, Sun Y, Hu L, Sun B, Trent J, et al. APEX1 gene amplification and its protein overexpression in osteosarcoma: correlation with recurrence, metastasis, and survival. *Technol Cancer Res Treat* 2010; 9:161-9; PMID:20218738; <http://dx.doi.org/10.1177/153303461000900205>
- [55] Paglin S, Hollister T, Delohery T, Hackett N, McMahon M, Sphicas E, Domingo D, Yahalom J. A novel response of cancer cells to radiation involves autophagy and formation of acidic vesicles. *Cancer Res* 2001; 61:439-44; PMID:11212227
- [56] Backues SK, Chen D, Ruan J, Xie Z, Klionsky DJ. Estimating the size and number of autophagic bodies by electron microscopy. *Autophagy* 2014; 10:155-64; PMID:24270884; <http://dx.doi.org/10.4161/auto.26856>